

Generalized quasi-geostrophy for spatially anisotropic rotationally constrained flows

By KEITH JULIEN¹, EDGAR KNOBLOCH²,
RALPH MILLIFF³ AND JOSEPH WERNE³

¹Department of Applied Mathematics, University of Colorado, Boulder, CO 80309, USA

²Department of Physics, University of California, Berkeley, CA 94720, USA

³Colorado Research Associates Division, NorthWest Research Associates, Boulder, CO 80301, USA

(Received 28 June 2004 and in revised form 28 October 2005)

Closed reduced equations analogous to the quasi-geostrophic equations are derived in the extratropics for small Rossby numbers and vertical scales that are comparable to or much larger than horizontal scales. On these scales, significant vertical motions are permitted and found to couple to balanced geostrophic dynamics. In the equatorial regions, similar reduced equations are derived for meridional scales much larger than the vertical and zonal scales. These equations are derived by a systematic exploration of different aspect ratios, and Froude and buoyancy numbers, and offer advantages similar to the standard quasi-geostrophic equations for studies of smaller-scale processes and/or of the equatorial regions.

1. Introduction

The quasi-geostrophic (QG) approximation (Charney 1948, 1971) to the equations of motion has served as a foundation for geophysical fluid dynamical theory and numerical experimentation for several decades. The QG balance is appropriate for geophysical flows wherein the effects of planetary rotation dominate all other time and space scales. This approximation therefore focuses attention on daily and longer time scales, and on spatial scales comparable to large fractions of the planetary scale. The approximation is based on the smallness of a parameter called the Rossby number (Ro) that measures the relative importance of the inertial and rotation terms in the momentum balance. Classical texts (Pedlosky 1979; Salmon 1998) derive the QG balance as the reduced equations that arise at first order in an asymptotic expansion of the equations of motion in powers of Ro .

The resulting equations possess certain conservation properties that lead to deep insights in geophysical fluid dynamics. Kinetic and potential energies can be derived for the QG equations (QGE) that are consistent with the asymptotic expansion, and are conserved in sum, at the same order in Rossby number as the prognostic equations. Other properties conserved to $O(Ro)$ in the QG balance include mass, momentum and buoyancy; see §2.1. The QGE form the simplest system of equations that support the free evolution of baroclinic instability and the consequent eddy dynamics, and include exchanges between kinetic and potential energies. Importantly, the evolution of the characteristic wave modes of the QG balance (the so-called vortical modes or Rossby waves) is not affected by wave modes with faster characteristic time scales such as inertial or gravity waves that may dominate the variability in measurements

of real geophysical fluids. This time and space scale separation leads to significant efficiencies in numerical implementations of the QGE as well.

While classical quasi-geostrophy is formally identified with small Rossby number, the ‘thin-layer’ approximation also enters the scaling for vertical velocity. In this approximation, the horizontal scales are assumed to be much larger than vertical scales, and as a result the QG vertical velocity is in fact much smaller than even $O(Ro)$. However, despite its unquestioned success in describing flows satisfying these assumptions, there are circumstances in geophysical fluid dynamics where these assumptions are inappropriate and the QG approximation does not apply. This is the case for flows that are dominated by $O(1)$ vertical processes. For instance, in open-ocean deep convection, vigorous downwelling plumes are observed with vertical velocities $\sim 10 \text{ cm s}^{-1}$, horizontal scales $\lesssim 1 \text{ km}$ and vertical scales of the order of several kilometres. Such anisotropic structures may be rotationally constrained, i.e. $Ro \lesssim 1$ (Marshall & Schott 1999). Although the case for anisotropic rotationally constrained flows of this type in the atmosphere is less compelling, atmospheric deep convection is a common phenomenon in the tropics. These observations suggest two questions. (i) Are there extensions of QGE that are appropriate on these smaller scales? (ii) What reduced equations can be obtained as the eddy motion scale is varied systematically from large to small, while respecting the requirement $Ro \ll 1$ appropriate for rapidly rotating flows? Julien, Knobloch & Werne (1998a) answer the former question in the affirmative; the latter is the subject of the present work.

In this paper we extend the asymptotic expansion of the equations of motion in Ro to include a variety of anisotropic scalings in the horizontal and vertical. This procedure leads to a catalogue of reduced systems of equations that are appropriate for large-scale geophysical fluid motions in the sense of QG, but are specific to anisotropies in the spatial scales that might be essential to particular geophysical fluid regimes. We are primarily motivated by asymptotic balances appropriate for the Earth’s atmosphere and oceans. One important byproduct of our approach is a reduced equation description of the equatorial region through a β -plane approximation and projection on the horizontal component of planetary rotation. In classical QG the equatorial region is formally excluded since the Rossby number is defined in terms of the local vertical component of rotation; this component vanishes at the equator. This observation leads naturally to the consideration of anisotropic scaling for the equatorial regions, a point emphasized most recently by Majda & Klein (2003).

This paper is organized as follows. In §2 we summarize the basic equations and dimensionless parameters of the problem. We also introduce the anisotropic scaling of the equations used in subsequent sections, and identify the conditions under which different components of the rotation vector dominate the dynamics. Section 3 provides a summary of our results. In particular, §3 contains tables summarizing the parameter regimes for which reduced QG equations have been found (table 3) and the resulting QGE (table 4). Asymptotic derivations of these equations follow in §§4–6. In §4 we focus on the ‘thin-layer’ regime and derive reduced equations valid in the extratropical regions. In §5, we introduce the so-called tilted quasi-hydrostatic quasi-geostrophic equations (TQH-QGE; Embid & Majda 1998) in which the ‘thin-layer’ approximation is relaxed, and more significant vertical motions are permitted. Appropriate forms of these equations valid away from and near the equator are derived. Finally, in §6 we consider the columnar or plume-like regimes. Remarkably, it is found that the classical QGE and the TQH-QGE can be extended into this regime provided the spatial anisotropy is not too great. Ultimately, a non-hydrostatic regime is entered. Here, too, reduced equations can be obtained; these are valid in the extratropical

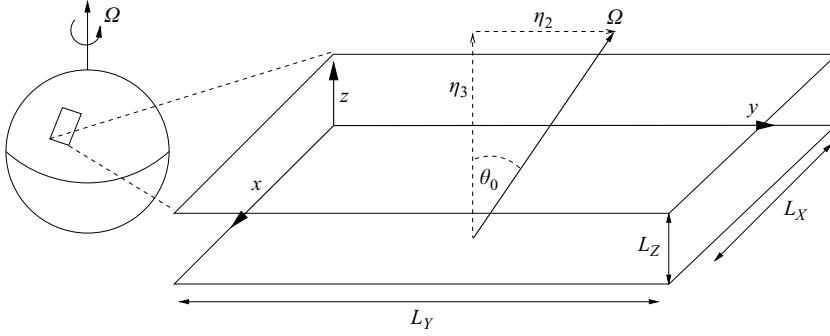


FIGURE 1. Schematic of the plane parallel geometry extracted from a spherical fluid layer.

regions and we refer to them as the non-hydrostatic quasi-geostrophic equations (NH-QGE).

Throughout, the focus of the paper is on the derivation of the different types of reduced equations, and not on their consequences, although some of their conservation properties are noted in Appendix B. It turns out that reduced equations exist only in certain parameter regimes, and it is these that are identified in this paper. Detailed consequences of the new equations will be explored in a future publication. Some of the more mathematical details of the derivations are given in Appendix A.

2. Problem formulation and preliminaries

As illustrated schematically in figure 1, we neglect the effects of sphericity and adopt a local right-handed Cartesian coordinate system $\mathbf{x}^* = (x^*, y^*, z^*)$ on the surface of a sphere of radius R at colatitude ϑ_0 and longitude ϕ . Here $\mathbf{x}^* = (x^*, y^*, z^*) \equiv R(\phi, \vartheta_0 - \vartheta, r/R - 1)$, so that x^* points eastward, y^* northward and z^* radially. The domain size is given by $L_X \times L_Y \times L_Z$. The total planetary rotation vector is given by $2\Omega\hat{\boldsymbol{\eta}}$ with unit direction $\hat{\boldsymbol{\eta}} := (0, \sin(\vartheta_0 - y^*/R), \cos(\vartheta_0 - y^*/R))$. Fluid motions are further restricted to a β -plane appropriate when $y^*/R \ll 1$. Specifically, we write $\hat{\boldsymbol{\eta}} \approx \hat{\boldsymbol{\eta}}_0 - (y^*/R)\hat{\boldsymbol{\eta}}_1$ with $\hat{\boldsymbol{\eta}}_0 := (0, \eta_2, \eta_3) \equiv (0, \sin \vartheta_0, \cos \vartheta_0)$ and $\hat{\boldsymbol{\eta}}_1 := (0, \eta_3, -\eta_2)$.

In a rotating stratified fluid layer the pressure and density fields may be decomposed into an ambient stratification profile (denoted by an overbar), and a fluctuating component arising as a consequence of fluid motion (denoted by a prime):

$$p^* = \bar{p}^*(z^*) + p'^*(\mathbf{x}^*, t^*), \quad \rho^* = \bar{\rho}^*(z^*) + \rho'^*(\mathbf{x}^*, t^*). \quad (2.1)$$

Asterisks denote quantities in dimensional form. In the absence of fluid motions ($\mathbf{u}^* = 0$) the fluid layer satisfies hydrostatic balance,

$$\partial_{z^*} \bar{p}^* = -g \bar{\rho}^*, \quad (2.2)$$

where g is the acceleration due to gravity and z denotes the local vertical coordinate. Within the Boussinesq approximation, the equations governing fluid motion are

$$D_t^* \mathbf{u}^* + 2\Omega \hat{\boldsymbol{\eta}} \times \mathbf{u}^* = -\frac{1}{\rho_r^*} \nabla^* p' + b^* \hat{\mathbf{z}} + \mathcal{S}_{\mathbf{u}^*}, \quad (2.3a)$$

$$D_t^* b^* - \frac{g}{\rho_r^*} w^* \partial_{z^*} \bar{\rho}^* = \mathcal{S}_{b^*}, \quad (2.3b)$$

$$\nabla^* \cdot \mathbf{u}^* = 0, \quad (2.3c)$$

where $D_{t^*} := \partial_{t^*} + \mathbf{u}^* \cdot \nabla^*$ is the material derivative. Here $\mathbf{u}^* := (u^*, v^*, w^*)$ denotes the velocity field, and $b^* := -g\rho^*/\rho_r^*$ is the buoyancy anomaly field associated with density fluctuations ρ^* about the ambient density profile $\bar{\rho}^*$. The quantity ρ_r^* is a reference density. In (2.3a) and (2.3b) the terms \mathcal{S}_{u^*} and \mathcal{S}_{b^*} represent contributions from sources and sinks resulting from external forcing, molecular diffusion, and subgrid-scale motions. In general, buoyancy (or density) anomalies depend on one or more thermodynamic quantities which must be specified through an equation of state. These include temperature and salinity for ocean systems, and temperature and relative humidity for atmospheric systems. However, since there is, in fact, no need to specify the origin of buoyancy anomalies, the discussion that follows is kept as general as possible.

Throughout the various explorations of rotationally constrained flows in §§4–6, we assume that the dynamics of interest are characterized by a horizontal (zonal) length scale $L_x = L$, a (zonal) velocity scale U , a buoyancy anomaly scale $B = g|\delta\rho^*/\rho_r^*|$, a dynamic pressure scale δp^* , and a reference density scale height H_ρ given by $H_\rho^{-1} = |(\partial_z \bar{\rho}^*)_r|/\rho_r^*$, where $(\partial_z \bar{\rho}^*)_r$ is a reference density gradient. Thus, if $\partial_z \bar{\rho}^*(z^*) < 0$ (> 0), the layer is stably (unstably) stratified. The (reference) stratification is characterized by the quantity $N_0 = \sqrt{g/H_\rho}$, representing the Brunt–Väisälä (or buoyancy) frequency when the layer is stably stratified. Using L , U , B , δp^* and $\delta\rho^*$ as the units for length, velocity, buoyancy anomaly, pressure and density, respectively, we recast the governing equations in non-dimensional form:

$$D_t \mathbf{u} + \frac{1}{Ro} \boldsymbol{\Omega}(y) \times \mathbf{u} = -P \nabla p + \Gamma b \hat{\mathbf{z}} + \mathcal{S}_u, \quad (2.4a)$$

$$D_t \left(b - \frac{1}{\Gamma Fr^2} \bar{\rho}(z) \right) = \mathcal{S}_b, \quad (2.4b)$$

$$\nabla \cdot \mathbf{u} = 0. \quad (2.4c)$$

Here $\boldsymbol{\Omega}(y) = \hat{\boldsymbol{\eta}}_0 - A_\beta y \hat{\boldsymbol{\eta}}_1$, where $A_\beta := L/R$ defines the scale of variation for the β -effect (with magnitude A_β/Ro) that occurs as a consequence of the latitudinal variation of the planetary rotation in a plane-parallel geometry. Non-dimensionalization also gives $\mathcal{S}_u = \mathcal{S}_{u^*} L/U^2$ and $\mathcal{S}_b = \mathcal{S}_{b^*} L/UB$. As an example of source/sink terms we consider the case of molecular (or eddy) diffusion

$$\mathcal{S}_u = \frac{1}{Re} \nabla^2 \mathbf{u}, \quad \mathcal{S}_b = \frac{1}{Pe} \nabla^2 b, \quad (2.5)$$

where $Re = UL/\nu$ and $Pe = UL/\kappa$ are the Reynolds and Péclet numbers. The additional non-dimensional parameters that appear are

$$\text{Rossby number: } Ro \equiv \frac{U}{2\Omega L} = \frac{T_\Omega}{T_U},$$

$$\text{Froude number: } Fr \equiv \frac{U}{N_0 L} = \frac{T_N}{T_U},$$

$$\text{Euler number: } P \equiv \frac{\delta p^*}{\rho_r^* U^2},$$

$$\text{Buoyancy number: } \Gamma \equiv \frac{BL}{U^2}.$$

The first two of these, Ro and Fr , can be interpreted in terms of ratios of characteristic time scales. These are the dynamical or eddy turnover time $T_U = L/U$, the planetary

rotation time $T_\Omega = 1/2\Omega$, and the buoyancy time $T_N = 1/N_0$. The last two, P and Γ (Embid & Majda 1998), represent the magnitudes of the pressure gradient and buoyancy forces relative to the inertial ‘acceleration force’. Although both can be absorbed by rescaling p and b we choose not to do so in order to provide a quantitative comparison of the magnitude of pressure and buoyancy fluctuations in the different regimes identified in §§4–6. The ratio $Fr/Ro = 2\Omega/N_0$ specifies the characteristic frequency ratio for inertial and gravity waves. Furthermore, from (2.4b) the quantity \mathcal{F} , where

$$\mathcal{F}^2 := \Gamma Fr^2 = \frac{BL}{N_0^2 L^2}, \quad (2.6)$$

is a vertical Froude number based on the characteristic vertical free-fall velocity $(BL)^{1/2}$ on characteristic length scale L . Inspection of the total buoyancy,

$$\Pi := b - \frac{1}{\mathcal{F}^2} \bar{\rho}(z), \quad (2.7)$$

shows that this quantity measures the relative importance of buoyancy anomalies about the background stratification $\bar{\rho}(z)$; for strongly stably stratified fluids, $\mathcal{F} < 1$ and buoyancy fluctuations about the mean are small.

We remark that the present definition of Ro is based on the magnitude of the entire planetary rotation vector 2Ω as opposed to the commonly used definition based on the projected local vertical component $2\Omega \cos \vartheta_0$, (i.e. the Coriolis parameter). The latter procedure results in an unnecessary restriction on the colatitude in the derivation of any reduced description for rotationally constrained dynamics using Ro as a small parameter, a difficulty that does not arise in our formulation. Our formulation therefore permits an exploration of the reduced dynamics in the equatorial region as well.

In the following we assume that $Ro \ll 1$ and undertake a systematic exploration of the different reduced regimes arising from equations (2.4) as a function of the colatitude ϑ_0 . The characteristic spatial scales L , L_y and L_z of the slow dynamics play a crucial role and ultimately determine the distinguished relationships between Fr , P , Γ and Ro .

2.1. Conservation laws and invariants

When $\mathcal{S}_u = \mathcal{S}_b = A_\beta = 0$, the Boussinesq equations (2.4) conserve the potential vorticity $\omega_a \cdot \nabla \Pi$, the total buoyancy Π , as well as all functionals of $\omega_a \cdot \nabla \Pi$ and Π :

$$D_t(\omega_a \cdot \nabla \Pi) = 0, \quad D_t \Pi = 0, \quad D_t F(\omega_a \cdot \nabla \Pi) = 0, \quad D_t G(\Pi) = 0. \quad (2.8)$$

Here $\omega_a := \omega + \hat{\eta}_0/Ro$ is the absolute vorticity and $\omega := \nabla \times \mathbf{u}$ is the relative vorticity. In the Boussinesq approximation, conservation of potential vorticity following fluid elements is equivalent to conservation of volume of a fluid element because ω_a evolves as a line element and $\nabla \Pi$ evolves as a surface element. Inclusion of the β -effect results in

$$D_t(\omega_a \cdot \nabla \Pi) = -\frac{A_\beta}{Ro} \eta_3 \nabla \cdot (\mathbf{u} \Pi), \quad (2.9)$$

where now $\omega_a := \omega + \Omega(y)/Ro$. The forcing term on the right-hand side of this equation originates in the use of locally Cartesian coordinates; on a sphere, potential vorticity is conserved. However, as discussed further in Appendix B, this term is asymptotically negligible in all the rotationally constrained extratropical and tropical regimes considered here. In the following, we are therefore permitted to assume that potential vorticity (as defined above) is conserved at leading order, and hence that

it is a ‘slow’ variable, much as in systems experiencing balanced dynamics, such as geostrophy in stably stratified layers, where potential vorticity does not partake in fast (linear) gravity wave oscillations (Warn *et al.* 1995; Vallis 1996).

We can also identify conserved Eulerian quantities. With a rigid top and bottom we find that $d\langle E\rangle/dt = d\langle b\rangle/dt = 0$, where

$$\langle E\rangle \equiv \lim_{V \rightarrow \infty} \frac{1}{V} \int d\mathbf{x} \frac{1}{2}(\mathbf{u} \cdot \mathbf{u} + \Gamma(\Pi - z)^2), \quad \langle b\rangle \equiv \lim_{V \rightarrow \infty} \frac{1}{V} \int d\mathbf{x} b \quad (2.10)$$

are, respectively, the total energy based on available potential energy (Shepherd 1993) and the buoyancy anomaly, both averaged over a fixed volume V . For small-amplitude motions the former yields the relation

$$\frac{d}{dt} \langle E_S \rangle - \frac{1}{2} \Gamma^2 Fr^2 \left\langle w b^2 \frac{\partial_{zz} \bar{\rho}}{(\partial_z \bar{\rho}(z))^2} \right\rangle = 0, \quad (2.11)$$

where

$$\langle E_S \rangle \equiv \lim_{V \rightarrow \infty} \frac{1}{V} \int d\mathbf{x} \frac{1}{2} \left(\mathbf{u} \cdot \mathbf{u} - \Gamma^2 Fr^2 \frac{b^2}{\partial_z \bar{\rho}(z)} \right) \quad (2.12)$$

is the small-amplitude energy. Thus $\langle E_S \rangle$ is conserved in the following three circumstances: when (i) $\Gamma Fr \ll 1$, (ii) w is a higher-order quantity, or (iii) the density stratification is linear, $\bar{\rho}(z) = \alpha z$. A fourth possibility also arises: (iv) b may be independent of (x, y) at leading order. Since $\bar{w} = 0$ it follows that, in this case too, $\langle E_S \rangle$ will be conserved at leading order.

We mention, finally, that it is also possible to derive Lagrangian conserved quantities. For example, for a comoving volume V_L , the quantities

$$\langle E \rangle_L \equiv \frac{1}{V_L} \int d\mathbf{x} \frac{1}{2}(\mathbf{u} \cdot \mathbf{u} + \Gamma(\Pi - z)^2), \quad \langle b \rangle_L \equiv \frac{1}{V_L} \int d\mathbf{x} b \quad (2.13)$$

are both conserved. Any meaningful reduced system of equations must preserve these properties.

2.2. Geostrophy and quasi-geostrophy

Rotationally constrained flows with characteristic horizontal length scale L and velocity scale U are characterized by the time ordering

$$T_\Omega \lesssim T_U, \quad (2.14)$$

i.e. by $Ro \lesssim 1$. A particularly tractable regime arises when $Ro \ll 1$ and the dynamics decompose into fast inertial waves, propagating on an $O(Ro)$ time scale, and slow eddy motions, evolving on an $O(1)$ time scale. The former are omitted from further consideration; Embid & Majda (1998) show that such waves are nonlinearly decoupled from the slow eddy motions. For the slow motions, the standard balance is provided by geostrophy, a diagnostic relation between the Coriolis and pressure gradient forces, i.e.

$$Ro^{-1} \hat{\eta}_0 \times \mathbf{u} \approx -P \nabla p. \quad (2.15)$$

Thus $P \sim Ro^{-1}$ for the present spatially isotropic non-dimensionalization. In conjunction with the continuity equation (2.4c), it follows from (2.15) that

$$\hat{\eta}_0 \cdot \nabla \mathbf{u} \approx 0, \quad \hat{\eta}_0 \cdot \nabla p \approx 0. \quad (2.16)$$

This is the Taylor–Proudman constraint (Taylor 1923; Proudman 1916) requiring leading-order motions to be invariant along the axis of rotation. The axis of rotation

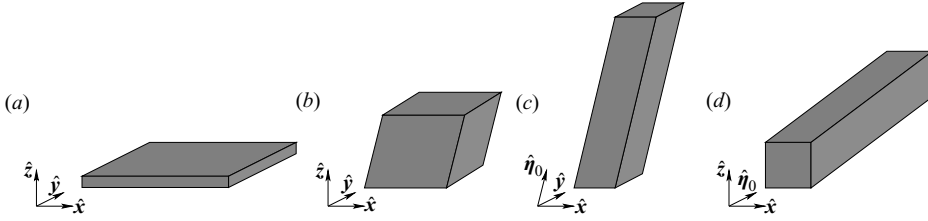


FIGURE 2. Fundamental domains employed in the anisotropic formulation. (a) Small aspect ratio $A_y := L_y/L = O(1)$, $A_z := L_z/L \ll 1$, (b) order one aspect ratio $A_y = O(1)$, $A_z = O(1)$, (c) large aspect ratio tilted $A_y = O(1)$, $A_z \gg 1$, (d) large aspect ratio equatorial $A_y \gg 1$, $A_z = O(1)$.

therefore plays a critical role in the dynamics of geostrophically balanced flows. In the absence of baroclinic forcing or inertial terms this two-dimensionalization of fluid motions constrains the bulk flow outside of any momentum boundary layers. This constraint is most naturally expressed in the non-orthogonal coordinate system defined by $\hat{x}, \hat{y}, \hat{\eta}_0$ with coordinates $(\tilde{x}, \tilde{y}, \eta)$: in this coordinate system equations (2.16) become $\partial_\eta \mathbf{u} = 0$, $\partial_\eta p = 0$. Thus, all solutions of the form

$$\mathbf{u} \approx -\nabla \times \Psi(\tilde{x}, \tilde{y}, t) \hat{\eta}_0 - \nabla \times \nabla \times \Phi(\tilde{x}, \tilde{y}, t) \hat{\eta}_0, \quad p \approx (RoP)^{-1} \Psi(\tilde{x}, \tilde{y}, t) \quad (2.17)$$

satisfy the constraint (2.15). The necessary vector relations and identities are listed in Appendix A. The linear rather than nonlinear dependence between pressure and velocity represents a key feature of geostrophy. Since the above coordinate system becomes degenerate in the tropics ($\hat{\eta}_0 \rightarrow \hat{y}$), an alternative coordinate representation $\hat{x}, \hat{\eta}_0, \hat{z}$ with coordinates $(\tilde{x}, \eta, \tilde{z})$ is also useful. The corresponding η -independent solution is given by

$$\mathbf{u} \approx -\nabla \times \Psi(\tilde{x}, \tilde{z}, t) \hat{\eta}_0 - \nabla \times \nabla \times \Phi(\tilde{x}, \tilde{z}, t) \hat{\eta}_0, \quad p \approx (RoP)^{-1} \Psi(\tilde{x}, \tilde{z}, t). \quad (2.18)$$

This coordinate system becomes degenerate at the poles ($\hat{\eta}_0 \rightarrow \hat{z}$).

Spatial modulation on scales $L_z \gtrsim L$ or $L_y \gtrsim L$ may also be included. These scales are typically required to incorporate boundary conditions on the scale L_z or the β -effect on the scale L_y . As a result equations (2.17) and (2.18) take the more general form

$$\mathbf{u} \approx -\nabla \times \Psi(\tilde{x}, \tilde{y}, Z, t) \hat{\eta}_0 - \nabla \times \nabla \times \Phi(\tilde{x}, \tilde{y}, Z, t) \hat{\eta}_0, \quad p \approx (RoP)^{-1} \Psi(\tilde{x}, \tilde{y}, Z, t), \quad (2.19)$$

where $Z \equiv z/A_z$, $A_z \equiv L_z/L$, and

$$\mathbf{u} \approx -\nabla \times \Psi(\tilde{x}, Y, \tilde{z}, t) \hat{\eta}_0 - \nabla \times \nabla \times \Phi(\tilde{x}, Y, \tilde{z}, t) \hat{\eta}_0, \quad p \approx (RoP)^{-1} \Psi(\tilde{x}, Y, \tilde{z}, t), \quad (2.20)$$

where $Y \equiv y/A_y$, $A_y \equiv L_y/L$. Both cases yield reduced dynamics, although no such dynamics were identified when both slow scales are present simultaneously.

In the absence of such larger scales the Taylor–Proudman constraint forces the trivial solution $\mathbf{u} = 0$ (or equivalently $\Psi = \Phi = 0$) by propagating the boundary condition $\hat{z} \cdot \mathbf{u} = 0$ on impenetrable horizontal boundaries into the interior. Departures from this constraint, consistent with impenetrable boundary conditions, can arise in several ways depending on the characteristic aspect ratio of the eddy motions (see figure 2). In the following we use the terminology large aspect ratio to refer to tall thin structures ($L, L_y \ll L_z$; figure 2c) or meridionally extended structures ($L, L_z \ll L_y$; figure 2d), while the terminology small aspect ratio will be reserved for horizontally extended structures ($L, L_y \gg L_z$; figure 2a). For large aspect ratio

structures (figure 2*c, d*) compliance with the Taylor–Proudman constraint requires the presence of large-scale spatial modulation. For small aspect ratio and order-one structures (figures 2*a, b*), such scales are not required, and the discussion that follows can be carried out in the local Cartesian coordinates (x, y, z) .

With buoyancy forcing included, equation (2.15) becomes

$$Ro^{-1}\hat{\eta}_0 \times \mathbf{u} \approx -P\nabla p + \Gamma b\hat{\mathbf{z}}. \quad (2.21)$$

Consequently, when $\Gamma \sim Ro^{-1}$ the Taylor–Proudman constraint is relaxed already at leading order, in favour of quasi-hydrostatic balance

$$-Ro^{-1}\eta_2 u \approx -P\partial_z p + \Gamma b \quad (2.22)$$

in the vertical, and the thermal wind balance

$$-Ro^{-1}\hat{\eta}_0 \cdot \nabla \mathbf{u}_\perp \approx \Gamma \nabla \times b\hat{\mathbf{z}} \quad (2.23)$$

in the horizontal. Here $\mathbf{u}_\perp \equiv (u, v, 0)$. The continuity equation together with impenetrable boundaries continues to imply that $\hat{\mathbf{z}} \cdot \mathbf{u} \approx 0$ throughout the layer. It follows that solutions to (2.21) take the reduced form

$$\mathbf{u} \approx \hat{\mathbf{z}} \times \nabla \Psi(x, y, z, t), \quad p \approx (RoP)^{-1}\eta_3 \Psi(x, y, z, t), \quad b \approx (Ro\Gamma)^{-1}\hat{\eta}_0 \cdot \nabla \Psi(x, y, z, t). \quad (2.24)$$

The above leading-order solution is appropriate for flows for which $L \gtrsim \max(L_y, L_z)$. For small aspect ratio flows for which $L \gg L_z$, $\hat{\eta}_0 \cdot \nabla \sim \eta_3 \partial_z$, and the resulting equations provide the standard description of rotationally constrained dynamics in a thin layer in the extratropical regions where $\hat{\eta}_0 \approx \eta_3 \hat{\mathbf{z}}$. For a stably stratified layer these prognostic equations describe geostrophically balanced slow-flow evolution, and have acquired the name ‘quasi-geostrophy’ (Charney 1948, 1971; Pedlosky 1979; Salmon 1998). For $L \sim L_z$ equations (2.24) are the prognostic equations for the slanted quasi-geostrophic equations introduced by Embid & Majda (1998).

In the tropics, where $\hat{\eta}_0 = \hat{\mathbf{y}}$, the Taylor–Proudman constraint operates in an orthogonal direction to $\hat{\mathbf{z}}$, and vertical motions on scale L are not impeded ($\hat{\mathbf{z}} \cdot \mathbf{u} \neq 0$). In this case an analogue of the classical quasi-geostrophic theory exists even in the absence of buoyancy forcing.

In the remaining subsections we identify the precise dependence of geostrophy on the spatial anisotropy as quantified by A_y , A_z and the colatitude ϑ_0 .

2.3. Anisotropic formulation

Table 1 contains quantitative information about the non-dimensional numbers referred to above for some relevant atmospheric and oceanic flows. It is clear from §1 and table 1 that one distinguishing measure of the different geophysical regimes is the degree of spatial anisotropy between the characteristic horizontal length scale L and the vertical length scale L_z (see rows 1, 2 and 4 of table 1). Inspection of table 1 also reveals that sphericity effects are important (i.e. $A_\beta \sim 1$) to general circulation in the atmosphere, a topic outside the scope of the present investigation. Moreover, atmospheric phenomena are generally sufficiently deep that effects of compressibility are likely to be important. In these circumstances the anelastic approximation (Bannon 1996) rather than the Boussinesq approximation to the Navier–Stokes equation becomes appropriate. Although the results of this paper can be generalized to this case, our purpose here is to enumerate clearly the different rotationally constrained regimes without the additional complication of non-Boussinesq effects.

To highlight the role of anisotropy we express (y, z) in units of (L_y, L_z) instead of L . In addition, we express (v, w) in units of $(L_y, L_z)U/L$. In terms of the aspect ratios

	Atmosphere General circulation	Atmosphere Synoptic	Ocean General circulation	Ocean Synoptic	Ocean Mesoscale	Ocean Plume
L, L_y (km)	10^4	10^3	10^3	50–100	10–50	0.6–1.5
L_z (km)	10^1	10^1	1–3	0.5–1	0.1–0.7	1–2
U (m s^{-1})	10	10	5×10^{-2} –1	0.4–1	0.1–0.4	0.1
$A_z^{-1} = L/L_z$	10^3	10^2	10^3	10^2	10^1 – 10^2	10^{-1} –1
$A_\beta = L_y/R$	1.6	10^{-1}	10^{-1}	10^{-2}	10^{-3} – 10^{-2}	10^{-4}
$Ro = U/2\Omega L$	10^{-2}	10^{-1}	10^{-4} – 10^{-2}	10^{-2} – 10^{-1}	10^{-2} – 10^{-1}	10^{-1} –1
$Fr = U/ N_0 L$	10^{-4}	10^{-3}	10^{-6} – 10^{-4}	10^{-5} – 10^{-3}	10^{-4} – 10^{-3}	$\rightarrow \infty$
$\Gamma = BL/U^2 \dagger$	10^4	10^3	10^3 – 10^5	10^2 – 10^3	10^2 – 10^3	10 – 10^2
$ N_0 /2\Omega$	10^2	10^2	10^2	10^2	10^2	$\rightarrow 0$

(\dagger) indicates estimates based on $B \sim g\alpha\Delta T$ with $\alpha_{air} = 3.5 \times 10^{-3} \text{ K}^{-1}$, $\Delta T_{air} \sim 10 \text{ K}$ and $\alpha_{water} = 1.0 \times 10^{-4} \text{ K}^{-1}$, $\Delta T_{water} \sim 1 \text{ K}$. $R = 6378 \text{ km}$, $2\Omega = 1.4 \times 10^{-4} \text{ s}^{-1}$.

TABLE 1. Estimate of scales and dimensionless numbers characteristic of different geophysical regimes.

$A_y = L_y/L$, $A_z = L_z/L$ (recall $A_x \equiv L_x/L = 1$) the governing equations (2.4a)–(2.4c) become

$$D_t u + \frac{1}{Ro}(A_z(\eta_2 - A_\beta A_y y \eta_3)w - A_y(\eta_3 + A_\beta A_y y \eta_2)v) = -P \partial_x p + \mathcal{S}_u, \quad (2.25a)$$

$$A_y D_t v + \frac{1}{Ro}(\eta_3 + A_\beta A_y y \eta_2)u = -\frac{P}{A_y} \partial_y p + \mathcal{S}_v, \quad (2.25b)$$

$$A_z D_t w - \frac{1}{Ro}(\eta_2 - A_\beta A_y y \eta_3)u = -\frac{P}{A_z} \partial_z p + \Gamma b + \mathcal{S}_w, \quad (2.25c)$$

$$D_t \left(b - \frac{1}{\Gamma Fr^2} \bar{\rho}(z) \right) = \mathcal{S}_b, \quad (2.25d)$$

$$\nabla \cdot \mathbf{u} = 0. \quad (2.25e)$$

Here x, y, z and the associated derivatives ∇ refer to the stretched coordinates, i.e. all derivatives are of order one. Likewise all velocity components are nominally of the same order, $\mathbf{u} = O(1)$; the energies (2.10a), (2.13a) are modified accordingly. In the following we use equations (2.25) to identify three distinct regimes characterized by geostrophic balance, depending on whether the dominant component of the Coriolis force arises from the vertical, horizontal or both components of the rotation vector. These regimes are referred to as ‘[U]pright’ (figure 2a), ‘[S]ideways’ (figure 2d), or ‘[T]ilted’ geostrophy (figures 2b, c), respectively, and represent an extension of the classical case of upright geostrophy treated in the QG literature. By definition, upright geostrophy holds at the poles ($\eta_2 = 0$, $\eta_3 = \pm 1$), while sideways geostrophy holds at the equator ($\eta_2 = 1$, $\eta_3 = 0$); however, under appropriate conditions (see below) upright geostrophy characterizes moderate latitudes as well. A similar statement applies to sideways geostrophy.

In the remainder of this subsection we derive the conditions that define each of these regimes. The results are summarized in table 2. The upright and tilted regimes overlap in latitude (column 2) but are distinguished by their spatial anisotropy (columns 3 and 4). Upright geostrophy cannot occur in the equatorial region. Similarly, sideways geostrophy is not permitted in the polar regions.

Geostrophy	ϑ_0	A_y	A_z	A_β	P	Γ
Upright	$< \frac{1}{2}\pi - O(Ro)$	~ 1	$\min[1, o(\cot \vartheta_0)]$	$o(1)$	$\sim \frac{\cos \vartheta_0}{Ro}$	$o\left(\frac{P}{A_z}\right)$
Tilted	~ 1	~ 1	~ 1	$o(1)$	$\sim \frac{1}{Ro}$	$o(P)$
Sideways	$> O(Ro)$	$\min[1, o(\tan \vartheta_0)]$	~ 1	$o(1)$	$\sim \frac{\sin \vartheta_0}{Ro}$	$o(P)$

TABLE 2. Parameters corresponding to upright, tilted and sideways geostrophy [$\hat{\eta}_0 \equiv (0, \eta_2, \eta_3) = (0, \sin \vartheta_0, \cos \vartheta_0)$]. We adopt the notation $a(Ro) = o(\delta)$ as a shorthand for $\lim_{Ro \rightarrow 0} |a(Ro)/\delta| = 0$.

2.3.1. *Upright geostrophy*

Inspection of the governing equations (2.25a)–(2.25c) shows that the vertical component of the rotation dominates whenever $P \sim O(A_y \eta_3 / Ro)$ and[†]

$$\frac{A_z \eta_2}{A_y \eta_3} = o(1). \tag{2.26}$$

For leading-order geostrophic balance, the horizontal inertial acceleration terms in (2.25a) and (2.25b) must also be subdominant. Thus

$$\frac{Ro}{A_y \eta_3} = o(1), \quad \frac{A_y Ro}{\eta_3} = o(1). \tag{2.27}$$

It follows that $Ro/\eta_3 = o(1)$ [‡] and $A_y \sim 1$. As a consequence of this result the inertial acceleration terms in (2.25c) are automatically subdominant compared to the pressure gradient and bounded by

$$\frac{A_z^2 Ro}{A_y \eta_3} = o(1). \tag{2.28}$$

Likewise the β -effect is subdominant provided $A_\beta \eta_2 = o(1)$, a condition that is satisfied provided that $A_\beta = o(1)$, while the buoyancy term is subdominant provided

$$\Gamma = o(\eta_3 A_y / A_z Ro). \tag{2.29}$$

The implications of these constraints are summarized in table 2, row 1. In particular the upper bound for the aspect ratio A_z decreases monotonically from $A_z = 1$ in the polar region where $\vartheta_0 = O(Ro)$ to $A_z = o(Ro)$ as the tropics are approached, i.e. as $\vartheta_0 \rightarrow \pi/2 - O(Ro)$. Consistent with these constraints we make the choice

$$A_y = 1, \quad A_z = \min[1, o(\cot \vartheta_0)], \quad A_\beta = o(1), \quad P = \frac{1}{Ro}, \quad \Gamma = o\left(\frac{1}{A_z Ro}\right). \tag{2.30}$$

From equations (2.25) it now follows that the leading-order balance is one of upright geostrophy and horizontal non-divergence:

$$\eta_3 \hat{z} \times \mathbf{u}_{0\perp} = -\nabla p_0, \tag{2.31a}$$

$$\nabla_\perp \cdot \mathbf{u}_{0\perp} = 0. \tag{2.31b}$$

[†] The notation $a(\epsilon) = o(1)$ means that $a \rightarrow 0$ as $\epsilon \rightarrow 0$.

[‡] We note that Ro/η_3 is the Rossby number based on the Coriolis parameter $2\Omega \cos \vartheta_0$. It is this quantity that is typically used as the expansion parameter. Since this quantity is not small when $\eta_3 \ll 1$, upright dynamics are bounded away from the tropical region.

Here $\mathbf{u}_{0\perp} = (u_0, v_0, 0)$, and $\nabla_{\perp} = (\partial_x, \partial_y, 0)$ denotes the gradient in the plane perpendicular to the rotation vector $\hat{\mathbf{z}}$. Thus

$$\hat{\mathbf{z}} \cdot \nabla \mathbf{u}_{0\perp} = 0, \quad \hat{\mathbf{z}} \cdot \nabla p_0 = 0. \quad (2.32)$$

The QGE that describe the reduced dynamics consistent with this balance are summarized in § 3 and derived in § 4.

2.3.2. Sideways geostrophy

Following a line of argument similar to that presented above, we find that the horizontal component of rotation dominates provided $P \sim O(A_z \eta_2 / Ro)$ and

$$\frac{A_y \eta_3}{A_z \eta_2} = o(1), \quad (2.33)$$

while the inertial acceleration terms in (2.25a) and (2.25c) are subdominant provided

$$\frac{Ro}{A_z \eta_2} = o(1), \quad \frac{A_z Ro}{\eta_2} = o(1). \quad (2.34)$$

Thus $Ro/\eta_2 = o(1)^\dagger$ and $A_z \sim 1$. The constraints (2.33) and (2.34) define the sideways geostrophic balance, and their implications are summarized in table 2, row 3. Note that sideways geostrophy is achieved only in the extratropical and tropical regions, and that the upper bound for the aspect ratio A_y decreases monotonically from $A_y \sim 1$ in the tropics to $A_y = o(Ro)$ in the polar region. In addition the β -effect is subdominant provided $A_\beta A_y \eta_3 = o(1)$, a condition that is automatically satisfied, while the inertial term in (2.25b) is subdominant compared with the meridional pressure gradient whenever

$$\frac{A_y^2 Ro}{A_z \eta_2} = o(1). \quad (2.35)$$

Finally, the buoyancy term in equation (2.25c) is small compared with the horizontal Coriolis term provided that $\Gamma = o(\eta_2 / Ro)$. The choice

$$A_y = \min[1, o(\tan \vartheta_0)], \quad A_z = 1, \quad A_\beta = o(1), \quad P = \frac{1}{Ro}, \quad \Gamma = o\left(\frac{\eta_2}{Ro}\right) \quad (2.36)$$

results in leading-order sideways geostrophic balance and zonal-vertical non-divergence:

$$\eta_2 \hat{\mathbf{y}} \times \mathbf{u}_{0\perp} = -\nabla p_0, \quad (2.37a)$$

$$\nabla_{\perp} \cdot \mathbf{u}_{0\perp} = 0. \quad (2.37b)$$

Here \perp denotes the plane perpendicular to the rotation vector $\hat{\mathbf{y}}$ with $\mathbf{u}_{0\perp} = (u_0, 0, w_0)$ and $\nabla_{\perp} = (\partial_x, 0, \partial_z)$. The resulting motions are therefore non-hydrostatic, but satisfy the Taylor–Proudman constraint

$$\hat{\mathbf{y}} \cdot \nabla \mathbf{u}_{0\perp} = 0, \quad \hat{\mathbf{y}} \cdot \nabla p_0 = 0. \quad (2.38)$$

It turns out, however, that despite the large range of latitudes permitting sideways geostrophy, closed QGE describing the associated sideways reduced dynamics can only be derived for the tropics. On the other hand the resulting SNH-QGE constitute a limit of a broader class of reduced equations exhibiting tilted geostrophy that

[†] Ro/η_2 represents the complementary tropical Rossby number based on $2\Omega \sin \vartheta_0$. The requirement $Ro/\eta_2 \ll 1$ bounds sideways dynamics away from the polar region.

extends from the extratropics into the tropics and includes the β -effect. The latter are derived in § 6.2 using the multiple scale approach of § 2.3.4.

2.3.3. Tilted geostrophy

When rotation dominates the flow but both components are comparable we see that $P \sim O(A_y \eta_3 / Ro) \sim O(A_z \eta_2 / Ro)$. Thus

$$A_y \eta_3 \sim A_z \eta_2. \quad (2.39)$$

The inertial terms in (2.25a)–(2.25c) are subdominant provided

$$\frac{Ro}{A_y \eta_3} \sim \frac{A_y Ro}{\eta_3} \sim \frac{Ro}{A_z \eta_2} \sim \frac{A_z Ro}{\eta_2} = o(1). \quad (2.40)$$

These conditions imply that we may take the flow to be isotropic, $A_y, A_z = O(1)$, together with the requirement $Ro/\eta_3 = o(1)$, $Ro/\eta_2 = o(1)$, and hence that ϑ_0 must be bounded away from the pole and equator ($\eta_3 \sim \eta_2 \sim O(1)$). This condition is taken to define the extratropical regime. In this regime the β -effect is subdominant, and we require

$$\Gamma = o(1/Ro) \quad (2.41)$$

in order that buoyancy forcing is subdominant as well. The choice

$$A_y = 1, \quad A_z = 1, \quad A_\beta = o(1), \quad P = \frac{1}{Ro}, \quad \Gamma = o\left(\frac{1}{Ro}\right) \quad (2.42)$$

leads to geostrophic balance at leading order:

$$\widehat{\boldsymbol{\eta}}_0 \times \mathbf{u}_0 = -\nabla p_0, \quad (2.43a)$$

$$\nabla \cdot \mathbf{u}_0 = 0. \quad (2.43b)$$

Thus

$$\widehat{\boldsymbol{\eta}}_0 \cdot \nabla \mathbf{u}_0 = 0, \quad \widehat{\boldsymbol{\eta}}_0 \cdot \nabla p_0 = 0. \quad (2.44)$$

The QGE describing the resulting tilted reduced dynamics are summarized in § 3 and derived in § 5.

2.3.4. Multiple scale approach

Table 2 shows that when the layer is deep ($L_z \gg L$; figure 2c) or meridionally extended ($L_y \gg L$; figure 2d) the conditions for geostrophy on all scales fail. In such circumstances a different approach is required. In the following we continue to assume that geostrophy holds on $O(1)$ spatial scales. In these circumstances the Taylor–Proudman constraint tries to make the flow on the scale L independent of the coordinate along the rotation axis. The simplest way to deal with this constraint is to use the non-orthogonal coordinates mentioned in § 2.2. When boundary conditions are imposed at $z=0, L_z$ we introduce a large spatial scale $Z \equiv z/A_z$, $A_z = L_z/L \gg 1$, and write

$$\nabla \rightarrow \nabla + A_z^{-1} \widehat{\mathbf{z}} \partial_Z, \quad (2.45)$$

where ∇ is the gradient in the $(\tilde{x}, \tilde{y}, \eta)$ coordinates; † hereinafter upper case symbols denote modulational scales not constrained by geostrophy. With the

† Without loss of generality we assume that the small scale flow is isotropic ($A_y = A_z = 1$) even though table 2 shows that some anisotropy is permitted.

Taylor–Proudman constraint $\partial_\eta \equiv 0$ imposed, Appendix A, case A, implies that

$$\nabla = \widehat{\mathbf{x}}\partial_{\widehat{x}} + \widehat{\mathbf{y}}\frac{1}{\eta_3^2}\partial_{\widehat{y}} - \widehat{\boldsymbol{\eta}}_0\frac{\eta_2}{\eta_3^2}\partial_{\widehat{y}}. \quad (2.46)$$

This coordinate representation remains valid when $\vartheta_0 \lesssim \pi/2 - O(Ro)$, i.e. away from the tropics. Boundary conditions are imposed at $Z=0$ and $Z=1$.

For large-scale modulation in the meridional direction $\widehat{\mathbf{y}}$ required to include the β -effect we adopt the coordinates $(\widetilde{x}, \eta, \widetilde{z})$. A similar discussion now leads to (see Appendix A, case B)

$$\nabla \rightarrow \nabla + A_Y^{-1}\widehat{\mathbf{y}}\partial_Y, \quad \nabla = \widehat{\mathbf{x}}\partial_{\widehat{x}} - \widehat{\boldsymbol{\eta}}_0\frac{\eta_3}{\eta_2^2}\partial_{\widetilde{z}} + \widehat{\mathbf{z}}\frac{1}{\eta_2^2}\partial_{\widetilde{z}}, \quad (2.47)$$

with the modulation scale $Y \equiv y/A_Y$ now tied to the meridional direction; the β -effect is taken to operate on this scale, i.e. $A_\beta y \rightarrow A_\beta A_Y Y$, with $A_\beta A_Y = O(Ro)$. This coordinate representation becomes degenerate when $\vartheta_0 \lesssim O(Ro)$, i.e. near the poles.

In either case we decompose all variables into a large scale, slowly evolving mean component and a small scale, fluctuating component:†

$$\mathbf{v}(\mathbf{x}, X, t) = \overline{\mathbf{v}}(X, t) + \mathbf{v}'(\mathbf{x}, X, t), \quad (2.48)$$

where $\mathbf{v} := (\mathbf{u}, b, p)$ and $X := Y$ or Z as appropriate. The overbar denotes volume averaging over fast scales \mathbf{x} , i.e.

$$\overline{\mathbf{v}}(X, t) \equiv \lim_{V \rightarrow \infty} \frac{1}{V} \int_V \mathbf{v}(\mathbf{x}, X, t) d\mathbf{x}, \quad \overline{\mathbf{v}'} \equiv 0. \quad (2.49)$$

Assuming that the fluid is infinite in extent on the small spatial scales, these averages exist and are independent of the definition of the volume.

We find *a posteriori* situations where it is also necessary to introduce a slow time $T \equiv t/A_T$, $A_T \gg 1$, such that

$$\partial_t \rightarrow \partial_t + A_T^{-1}\partial_T. \quad (2.50)$$

In such cases the above decomposition must be extended to include a fast time average, i.e.

$$\mathbf{v}(\mathbf{x}, X, T) = \overline{\mathbf{v}}(X, T) + \mathbf{v}'_j(\mathbf{x}, X, t, T), \quad (2.51)$$

$$\overline{\mathbf{v}}(X, T) \equiv \lim_{V, \tau \rightarrow \infty} \frac{1}{V\tau} \int_{V, \tau} \mathbf{v}(\mathbf{x}, X, t, T) d\mathbf{x} dt. \quad (2.52)$$

The mean and fluctuating components of (2.4a)–(2.4c), written in non-orthogonal coordinates with velocity components $\mathbf{u} = (\widetilde{u}, \widetilde{v}, \widetilde{w})$ (recall that for $X = Z$, $\mathbf{u} = \widetilde{u}\widehat{\mathbf{x}} + \widetilde{v}\widehat{\boldsymbol{\eta}}_0$ and for $X = Y$, $\mathbf{u} = \widetilde{u}\widehat{\mathbf{x}} + \widetilde{v}\widehat{\boldsymbol{\eta}}_0 + \widetilde{w}\widehat{\mathbf{z}}$), are:

Mean

$$\left(\partial_t + \frac{1}{A_T}\partial_T\right)\overline{\mathbf{u}} + \frac{1}{A_X}\nabla_X \cdot (\overline{\mathbf{u}_X \mathbf{u}}) + \frac{1}{Ro}\boldsymbol{\Omega}(y) \times \overline{\mathbf{u}} = -\frac{P}{A_X}\nabla_X \overline{p} + \Gamma \overline{b\widehat{\mathbf{z}}} + \overline{\mathcal{S}_u}, \quad (2.53a)$$

$$\left(\partial_t + \frac{1}{A_T}\partial_T\right)\overline{b} + \frac{1}{A_X}\nabla_X \cdot \left(\overline{\mathbf{u}_X \left(b - \frac{1}{\Gamma Fr^2} \overline{\rho}\right)}\right) = \overline{\mathcal{S}_b}, \quad (2.53b)$$

$$\nabla_X \cdot \overline{\mathbf{u}_X} = 0; \quad (2.53c)$$

† No confusion with the notation in §2.0 is permitted.

Fluctuating

$$\begin{aligned} \left(D_t + \frac{1}{A_T} \partial_T + \frac{1}{A_X} \mathbf{u}_X \cdot \nabla_X \right) \mathbf{u}' + \frac{1}{A_X} \mathbf{u}'_X \cdot \nabla_X \bar{\mathbf{u}} - \frac{1}{A_X} \nabla_X \cdot (\overline{\mathbf{u}'_X \mathbf{u}'}) \\ + \frac{1}{Ro} \boldsymbol{\Omega}(y) \times \mathbf{u}' = -P \left(\nabla + \frac{1}{A_X} \nabla_X \right) p' + \Gamma b' \hat{\mathbf{z}} + \mathcal{S}'_u, \end{aligned} \tag{2.54a}$$

$$\begin{aligned} \left(D_t + \frac{1}{A_T} \partial_T + \frac{1}{A_X} \mathbf{u}_X \cdot \nabla_X \right) b' - \frac{1}{\Gamma Fr^2} \mathbf{u} \cdot \nabla \bar{\rho} - \frac{1}{A_X} \nabla_X \cdot \left(\mathbf{u}_X \left(b - \frac{1}{\Gamma Fr^2} \bar{\rho} \right) \right) \\ + \frac{1}{A_X} \mathbf{u}_X \cdot \nabla_X \left(\bar{b} - \frac{1}{\Gamma Fr^2} \bar{\rho} \right) = \mathcal{S}'_b, \end{aligned} \tag{2.54b}$$

$$\nabla \cdot \mathbf{u}' + \frac{1}{A_X} \nabla_X \cdot \mathbf{u}'_X = 0, \tag{2.54c}$$

where $\nabla_X = \hat{\mathbf{y}} \partial_Y$, $u_X = \hat{\mathbf{y}} \cdot \mathbf{u}$, $\bar{\rho} = \bar{\rho}(z)$ for $X = Y$, and $\nabla_X = \hat{\mathbf{z}} \partial_Z$, $u_X = \hat{\mathbf{z}} \cdot \mathbf{u}$, $\bar{\rho} = \bar{\rho}(Z)$ for $X = Z$. In addition, $D_t \equiv \partial_t + \mathbf{u} \cdot \nabla$. If time averaging is included we set $\partial_t \equiv 0$ in equations (2.53).

For $A_Z \gg 1$ and sufficiently small averaged source terms, $\overline{\mathcal{S}'_u} = o(1)$, equation (2.53a) implies that the fluid layer is on average in hydrostatic balance, $PA_Z^{-1} \partial_Z \bar{p} \approx \Gamma \bar{b}$, indicating that $\Gamma \sim PA_Z^{-1}$. This observation is used below to relate the scaling of P to that of Γ . Moreover, in this case the mean horizontal velocities are negligible, $\bar{\mathbf{u}} = o(1)$: with no net vertical mass flux, equation (2.53c) implies that $\bar{w} = 0$ so that the Coriolis force $Ro^{-1} \eta_3 (-\bar{v} \hat{\mathbf{x}} + \bar{u} \hat{\mathbf{y}})$ must be balanced by the Reynolds stress or source terms. Thus $(\bar{u}, \bar{v}) \sim (\max[RoA_Z^{-1}, Ro|\overline{\mathcal{S}'_u}]) = o(1)$. Identical estimates for the mean velocity obtain when $X = Y$. As a result we can set $\bar{\mathbf{u}} = 0$ in the fluctuating equations (2.54) and omit (2.53) from further consideration, providing a substantial simplification of the derivation of the reduced equations.

In the remainder of the paper we systematically explore the consequences of spatial anisotropy as quantified by the parameters A_y, A_z, A_Y, A_Z in equations (2.25) or the multiple-scale fluctuating equations (2.54) to derive a variety of reduced PDEs for rotationally constrained dynamics. We do so by relating the non-dimensional parameters $(\Gamma, Fr, P, A_y, A_z, A_X, A_\beta, A_T)$, as well as the colatitude ϑ_0 , to the expansion parameter $Ro \equiv \epsilon \ll 1$, and employing asymptotic expansions of the form

$$\mathbf{v} = \mathbf{v}_0 + \epsilon \mathbf{v}_1 + \epsilon^2 \mathbf{v}_2 + \dots, \tag{2.55}$$

or, in some cases, expansions in two small parameters ϵ, δ , where δ is a suitable measure of the aspect ratio A_X . The parameter relations are selected so as to recover geostrophic balance at leading order in this expansion; the balances at subsequent order provide the required reduced equations describing the evolution of the system within the constraint of the corresponding geostrophic balance. Only in certain regimes are these equations closed. These are summarized in §3 and derived in §§4–6. New classes of reduced quasi-geostrophic equations valid in extratropical and tropical regions for non-hydrostatic motions on the β -plane are identified, thereby extending the interpretation of ‘quasi-geostrophy’ in an asymptotically precise manner. Moreover, as mentioned in §2.1, any meaningful reduced dynamics must conserve both potential vorticity and energy in the inviscid, unforced limit. We refer to evolution equations with these properties as *dynamically consistent*. This paper identifies the regimes where this is the case. Our asymptotic analysis therefore leads to a universal description of rotationally constrained flows, both away from the equator and near it.

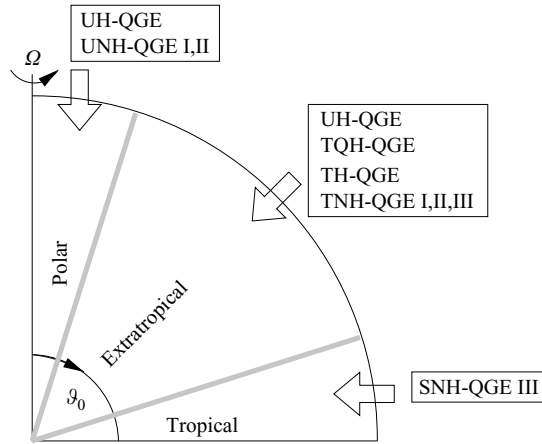


FIGURE 3. Classification of the reduced U–Upright, T–Tilted, S–Sideways QG models (see table 4) as a function of the colatitude ϑ_0 . H–hydrostatic, QH–quasi-hydrostatic, NH–non-hydrostatic, QG–quasi-geostrophic. Types I, II, and III denote [U,T]NH-QGE subclasses with distinct parameters (see table 3).

3. Summary of generalized quasi-geostrophy

In this section we summarize for convenience the reduced QGE derived in subsequent sections using a systematic asymptotic analysis of the effects of spatial anisotropy. Such a summary facilitates comparison among the different regimes; readers not interested in the details of the derivations can skip §§4–6.

Figure 3 summarizes the different regimes as a function of colatitude (cf. table 2), while figure 4 summarizes the transitions between them as a function of spatial anisotropy. The non-dimensional parameters corresponding to these regimes are given in table 3 and are consistent with the requirements of table 2 and the estimates of table 1. These regimes are distinguished by the relative size of Ro , the magnitude of the aspect ratios A_y, A_z (as indicated in figure 4), as well as the strength of the initial background stratification measured by \mathcal{F} . Closed sets of reduced equations are only found for Froude numbers Fr and \mathcal{F} that are not too large; the corresponding upper bounds are indicated in table 3. Hydrostatic and quasi-hydrostatic motions generally occur for $\mathcal{F} \leq O(Ro^{1/2})$, whereas non-hydrostatic motions occur for $\mathcal{F} \gtrsim O(Ro^{1/2})$.

The QGE that result are given in table 4. Since the reduced QGE appropriate in the extratropics transition smoothly, under appropriate conditions, into the corresponding equations valid in the polar and tropical regions (figure 4), these limiting cases are omitted. The six distinct regimes that result are labelled as either hydrostatic [H], quasi-hydrostatic [QH], or non-hydrostatic [NH]. For [QH] the Coriolis force enters the hydrostatic force balance; [NH] involves inertial terms in the vertical. Table 4 also specifies the coordinate system associated with each of the QGE. In the extratropical region, a non-orthogonal coordinate system is used to impose the Taylor–Proudman constraint on $O(L)$ scales whenever $L_y \gg L$ or $L_z \gg L$ (i.e. $A_y \gg 1$ or $A_z \gg 1$ in figure 4). For each class of QGE in table 4, the equation ‘*a*’ indicates the leading-order solution to the geostrophic force balance identified as upright (U), tilted (T) or sideways (S). A notable feature in all cases is the dynamic pressure which plays the role of the geostrophic streamfunction Ψ_0 that determines the fluid motion in planes perpendicular to the rotation axis. Subsequent equations in table 4 (i.e. ‘*b*’ to ‘*e*’, depending on the case) give the prognostic QGE. In all cases the inertial terms in the

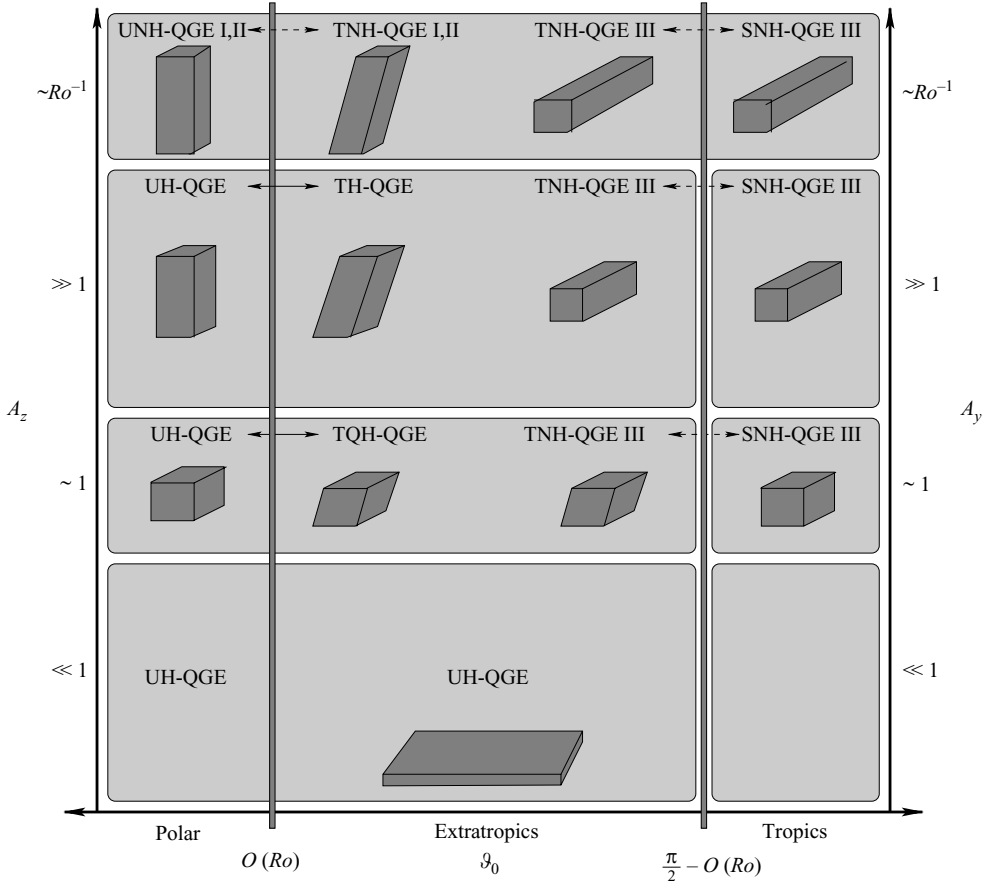


FIGURE 4. Classification of the reduced U–Upright, T–Tilted, S–Sideways QG models (see table 4) as a function of the colatitude ϑ_0 , and the spatial aspect ratios A_z or A_y . H–hydrostatic, QH–quasi-hydrostatic, NH–non-hydrostatic. With the exception of TNH-QGE III A_z distinguishes between all models in the polar and extratropical regions where $A_y = O(1)$, while A_y distinguishes between the tropical QGE and TNH-QGE III for which $A_z = O(1)$. The symbol \longleftrightarrow indicates a continuous transition between different models while \dashleftarrow indicates extension of a model to the polar or equatorial regions.

horizontal dominate material advection, $D_t^0 = \partial_t + \mathbf{u}_0 \cdot \nabla_{\perp}$, as expected of geostrophy. For the non-orthogonal coordinate representation $\mathbf{u}_0 \cdot \nabla_{\perp} = \tilde{u}_0 \partial_{\tilde{x}} + \tilde{v}_0 \partial_{\tilde{y}}$ for $X = Z$ and $\mathbf{u}_0 \cdot \nabla_{\perp} = \tilde{u}_0 \partial_{\tilde{x}} + \tilde{w}_0 \partial_{\tilde{z}}$ for $X = Y$.

In the remainder of this section we summarize the essential attributes of each regime, following the details presented in figure 4, and tables 3 and 4.

(a) *Small aspect ratio regime*

This regime occurs when $A_z = o(1)$, $A_y \sim 1$ (see figure 2a). The dominant contribution from the Coriolis force comes from the local vertical component $2\Omega\eta_3$. This assumption leads to an upright geostrophic balance and a description of the slow dynamics in the extratropical regions in terms of UH-QGE (table 4, equation (3.1)). The resulting QGE (schematically illustrated in figure 4) are derived in §4 for the parameter values given in table 3, and correspond to the classical equations of Charney (1948, 1971; see also Pedlosky 1979; Salmon 1998) that are valid for large-scale, stably

QGE	§	A_y	A_z	A_γ	A_z	A_β	A_T	P	Γ	Fr	\mathcal{F}
UH-QGE	4	1	$\min[1, o(\cot \vartheta_0)]$	–	–	Ro	–	Ro^{-1}	$(A_z Ro)^{-1}$	$\leq Ro A_z^{1/2}$	$\leq Ro^{1/2}$
TQH-QGE	5	1	1	–	–	Ro	–	Ro^{-1}	Ro^{-1}	$\leq Ro$	$\leq Ro^{1/2}$
TH-QGE	6.1.1	1	1	–	$o(Ro^{-1})$	$o(1)$	–	Ro^{-1}	$(A_z Ro)^{-1}$	$\leq Ro A_z^{1/2}$	$\leq Ro^{1/2}$
[U,T]NH-QGE I	6.1.2	1	1	–	Ro^{-1}	$o(1)$	–	Ro^{-1}	1	$\leq Ro^{1/2}$	$Ro^{1/2}$
[U,T]NH-QGE II	6.1.2	1	1	–	Ro^{-1}	$o(1)$	Ro^{-2}	Ro^{-2}	Ro^{-1}	$\leq Ro^{1/2}$	1
[T,S]NH-QGE III	6.2.1	$\min[1, \tan \vartheta_0]$	1	Ro^{-1}	–	Ro^{-2}	–	Ro^{-1}	1	1	1
[T,S]NH-QGE III no β -effect	6.2.1	–	1	$\in [1, Ro^{-1}]$	–	$o(Ro^{-1})$	–	Ro^{-1}	1	1	1

TABLE 3. Distinguished parameter values used in equations (2.25) or (2.53)–(2.54) to derive the QG models summarized in table 4. The letters U, T and S denote upright, tilted and sideways geostrophy, respectively (see figure 3 and table 2).

UH-QGE: (x, y, z, t)

$$\mathbf{u}_0 = \hat{\mathbf{z}} \times \nabla \Psi_0, \quad p_0 = \eta_3 \Psi_0, \quad b_0 = \eta_3 \partial_z \Psi_0 \quad (3.1a)$$

$$D_t^0 q_0 = -\eta_3 \partial_z \left(\frac{\mathcal{S}_b}{\partial_z \bar{\rho}(z)} \right) + \hat{\mathbf{z}} \cdot \nabla \times \mathcal{S}_{\mathbf{u}_\perp} \quad (3.1b)$$

$$q_0 = \nabla_\perp^2 \Psi_0 - \eta_3 \partial_z \left[\frac{\eta_3 \partial_z \Psi_0}{\partial_z \bar{\rho}(z)} \right] + \beta \eta_2 y \quad (3.1c)$$

TQH-QGE: (x, y, z, t)

$$\mathbf{u}_0 = \hat{\mathbf{z}} \times \nabla \Psi_0, \quad p_0 = \eta_3 \Psi_0, \quad b_0 = \hat{\boldsymbol{\eta}}_0 \cdot \nabla \Psi_0 \quad (3.2a)$$

$$D_t^0 q_0 = -\hat{\boldsymbol{\eta}}_0 \cdot \nabla \left(\frac{\mathcal{S}_b}{\partial_z \bar{\rho}(z)} \right) + \hat{\mathbf{z}} \cdot \nabla \times \mathcal{S}_{\mathbf{u}_{0\perp}} \quad (3.2b)$$

$$q_0 = \nabla_\perp^2 \Psi_0 - (\hat{\boldsymbol{\eta}}_0 \cdot \nabla) \frac{(\hat{\boldsymbol{\eta}}_0 \cdot \nabla) \Psi_0}{\partial_z \bar{\rho}(z)} + \beta \eta_2 y \quad (3.2c)$$

TH-QGE: $(\tilde{x}, \tilde{y}, Z, t)$

$$\mathbf{u}'_0 = -\nabla \times (\Psi_0 \hat{\boldsymbol{\eta}}_0 + \nabla \times \Phi_0 \hat{\boldsymbol{\eta}}_0), \quad p'_0 = \Psi_0, \quad b'_0 = \partial_Z \Psi_0 \quad (3.3a)$$

$$D_t^0 q_0 = -\eta_3^2 \partial_Z \left(\frac{\mathcal{S}_{b'_0}}{\partial_Z \bar{\rho}(Z)} \right) + \eta_3 \hat{\mathbf{z}} \cdot \nabla \times \mathcal{S}_{\mathbf{u}'_0} \quad (3.3b)$$

$$q_0 = \hat{\nabla}_\perp^2 \Psi_0 - \eta_3 \partial_Z \left[\frac{\eta_3 \partial_Z \Psi_0}{\partial_Z \bar{\rho}(Z)} \right] \quad (3.3c)$$

$$\nabla_\perp^2 \Phi_0 = \frac{\eta_2}{\eta_3} \partial_{\tilde{x}} \Psi_0 \quad (3.3d)$$

$$\hat{\nabla}_\perp^2 = \partial_{\tilde{x}}^2 + \partial_{\tilde{y}}^2 \quad (3.3e)$$

TNH-QGE I: $(\tilde{x}, \tilde{y}, Z, t)$

$$\mathbf{u}'_0 = -\nabla \times (\Psi_0 \hat{\boldsymbol{\eta}}_0 + \nabla \times \Phi_0 \hat{\boldsymbol{\eta}}_0), \quad p'_0 = \Psi_0, \quad (3.4a)$$

$$D_t^0 \nabla_\perp^2 \Psi_0 - \eta_3 \partial_Z \nabla_\perp^2 \Phi_0 = -\eta_2 \partial_{\tilde{x}} b'_0 + \hat{\boldsymbol{\eta}}_0 \cdot \nabla \times \mathcal{S}_{\mathbf{u}'_0} \quad (3.4b)$$

$$D_t^0 \nabla_\perp^2 \Phi_0 + \eta_3 \partial_Z \Psi_0 = \eta_3 b'_0 + \hat{\boldsymbol{\eta}}_0 \cdot \mathcal{S}_{\mathbf{u}'_0} \quad (3.4c)$$

$$D_t^0 b'_0 - (\eta_3 \nabla_\perp^2 \Phi_0 - \eta_2 \partial_{\tilde{x}} \Psi_0) \partial_Z \bar{\rho}(Z) = \mathcal{S}_{b'_0} \quad (3.4d)$$

TNH-QGE II: $(\tilde{x}, \tilde{y}, Z, t, T)$

$$\mathbf{u}'_0 = -\nabla \times (\Psi_0 \hat{\boldsymbol{\eta}}_0 + \nabla \times \Phi_0 \hat{\boldsymbol{\eta}}_0), \quad p'_0 = \Psi_0, \quad (3.5a)$$

$$D_t^0 \nabla_\perp^2 \Psi_0 - \eta_3 \partial_Z \nabla_\perp^2 \Phi_0 = -\eta_2 \partial_{\tilde{x}} b'_1 + \hat{\boldsymbol{\eta}}_0 \cdot \nabla \times \mathcal{S}_{\mathbf{u}'_0} \quad (3.5b)$$

$$D_t^0 \nabla_\perp^2 \Phi_0 + \eta_3 \partial_Z \Psi_0 = \eta_3 b'_1 + \hat{\boldsymbol{\eta}}_0 \cdot \mathcal{S}_{\mathbf{u}'_0} \quad (3.5c)$$

$$D_t^0 b'_1 + (\eta_3 \nabla_\perp^2 \Phi_0 - \eta_2 \partial_{\tilde{x}} \Psi_0) \partial_Z (\bar{b}_0 - \mathcal{F}^{-2} \bar{\rho}(Z)) = \mathcal{S}_{b'_1} \quad (3.5d)$$

$$\partial_T \bar{b}_0 + \partial_Z \overline{(\eta_3 \nabla_\perp^2 \Phi_0 - \eta_2 \partial_{\tilde{x}} \Psi_0) b'_1} = \epsilon^{-2} \overline{\mathcal{S}_{b_0}} \quad (3.5e)$$

TNH-QGE III: $(\tilde{x}, Y, \tilde{z}, t)$

$$\mathbf{u}'_0 = -\nabla \times (\Psi_0 \hat{\boldsymbol{\eta}}_0 + \nabla \times \Phi_0 \hat{\boldsymbol{\eta}}_0), \quad p'_0 = \Psi_0, \quad (3.6a)$$

$$D_t^0 \nabla_\perp^2 \Psi_0 - (\eta_2 \partial_Y + \beta \eta_2^{-1} Y \partial_{\tilde{z}}) \nabla_\perp^2 \Phi_0 = -\eta_2 \partial_{\tilde{x}} b'_0 + \hat{\boldsymbol{\eta}}_0 \cdot \nabla \times \mathcal{S}_{\mathbf{u}'_0} \quad (3.6b)$$

$$D_t^0 \nabla_\perp^2 \Phi_0 + (\eta_2 \partial_Y + \beta \eta_2^{-1} Y \partial_{\tilde{z}}) \Psi_0 = \eta_3 b'_0 + \hat{\boldsymbol{\eta}}_0 \cdot \mathcal{S}_{\mathbf{u}'_0} \quad (3.6c)$$

$$D_t^0 (b'_0 - \mathcal{F}^{-2} \bar{\rho}(z)) = \mathcal{S}_{b'_0} \quad (3.6d)$$

TABLE 4. Generalized QGE classified according to [U]pright or [T]ilted geostrophy (see table 2). In each case the solution to the geostrophic force balance is given in equation a , with the QGE given by the subsequent equations (see text). Tilted QGE are derived in non-orthogonal coordinates $\tilde{\mathbf{x}}, \tilde{\mathbf{y}}, \hat{\boldsymbol{\eta}}_0$ or $\tilde{\mathbf{x}}, \hat{\boldsymbol{\eta}}_0, \hat{\mathbf{z}}$ (see Appendix A), and transition to upright (sideways) subclasses upon $\hat{\boldsymbol{\eta}}_0 \rightarrow \hat{\mathbf{z}}$ ($\hat{\boldsymbol{\eta}}_0 \rightarrow \tilde{\mathbf{y}}$) which are omitted. The material derivative D_t^0 is defined by $D_t^0 = \partial_t + \mathbf{u}_0 \cdot \nabla_\perp$.

stratified hydrostatic motions in the low Ro , low Fr limit. Moreover, since $Fr/Ro \ll 1$, internal gravity waves in this regime propagate on a much faster time scale than inertial waves. However, with the exception of Rossby waves present owing to the β -effect, all wave motions are filtered out. A comparison between table 3, row 1, and table 1 shows that the resulting QGE are most relevant to synoptic-scale motions in the atmosphere and oceans, and basin-scale and mesoscale motions in the oceans.

In the polar regions, the β -effect drops out from the above QGE. However, the resulting equations have a much larger range of validity, and apply even when $A_z = o(Ro^{-1})$ (see (b) and (c) below and figure 4).

(b) *Intermediate aspect ratio regime*

This regime arises when $A_y \sim A_z \sim 1$ (see figure 2b), and leads to a description of the slow dynamics in the extratropical region in terms of TQH-QGE (table 4, equation (3.2)) and TNH-QGE III (table 4, equation (3.6) with the β -effect omitted). The TQH-QGE are derived in § 5 for the parameter values given in table 3. This system is a variant of the classical UH-QGE, valid in the low Ro , low Fr limit, for which the horizontal component of the Coriolis force $2\Omega\eta_2$ cannot be neglected (Embid & Majda 1998); as the polar regions are approached ($\hat{\eta}_0 \rightarrow \hat{z}$) these equations reduce to UH-QGE (figure 4). The TQH-QGE represent filtered dynamics despite the fact that $Fr/Ro \sim 1$, i.e. that inertial and gravity waves propagate on the same time scale.

Observations of step-like profiles in recent conductivity-temperature-density (CTD) measurements of open-ocean deep convection in the Labrador Sea have been attributed to the crossing of rotationally aligned vertical structures (Pickart, Torres & Clarke 2002). White & Bromley (1995) have speculated that the effect of the total Coriolis force becomes increasingly important as the equatorial region is approached. Thus, TQH-QGE may also be appropriate for mid-latitude mesoscale (see table 1) and sub-tropical dynamics where the horizontal component of the planetary rotation is larger than the vertical component.

The system TNH-QGE III (table 4, equation (3.6)), derived in § 6.2 for the parameter values given in table 3 (TNH-QGE III, last row), applies for weaker stratification ($Fr \sim 1$, so that $T_N \sim 1$). As a result gravity waves on an $O(L)$ scale or greater are permitted to propagate. This is so also for $O(L)$ wavelength inertial waves. When the β -effect is important TNH-QGE III permit fully non-hydrostatic β -plane motions (see (c) below). In the tropical regions a new class of quasi-geostrophic equations involving only the horizontal component of rotation can be derived. This system, referred to as SNH-QGE III (figure 4), can be deduced from its extratropical counterpart TNH-QGE III† characterized by tilted geostrophy on taking the limit $\hat{\eta}_0 \rightarrow \hat{y}$.

(c) *Large aspect ratio regime*

In this regime, the primary motions on $O(L)$ scales are columnar, and spatial modulation on large scales $Y = y/A_Y$, $A_Y \gg 1$ (see figure 2d), or $Z = z/A_Z$, $A_Z \gg 1$ (see figure 2c), must be included to take into account the β -effect or the presence of boundaries. The details depend on the degree of anisotropy (figure 4). For example, when $A_z = o(Ro^{-1})$ the QG dynamics in both polar and extra-tropical regimes are hydrostatic, and are described by UH-QGE and TH-QGE (table 4, equation (3.3)), derived in § 6.1.1 for the parameter values given in table 3. The TH-QGE are similar in functional form to the classical UH-QGE and the TQH-QGE of Embid & Majda (1998). However, in our case, the Taylor-Proudman constraint is enforced along

† The label III, as opposed to I, II, has been adopted for this reason.

the axis of rotation on the small scale L only, and buoyancy forcing requires the introduction of spatial modulation on the scale $L_z \gg L$ of the layer. The resulting equations filter out both internal gravity and inertial waves, and hence represent an extension of QG to the columnar regime. The TH-QGE transition smoothly to the UH-QGE in the polar regions.

In contrast, when $A_z = O(Ro^{-1})$ the slow dynamics are described by two new classes of [N]on-[H]ydrostatic QGE that are valid on the f -plane; since $A_y = 1$ the β -effect is negligible. We refer to these systems of equations as NH-QGE. The systems TNH-QGE I (table 4, equation (3.4)) and II (table 4, equation (3.5)) are derived in §6.1.2 for the parameter values given in table 3. Both systems transition smoothly to the corresponding upright version near the polar regions (figure 4). For type I, $\mathcal{F} = o(1)$ and the initial mean stratification remains unaltered by the fluid motions. However, for type II, $\mathcal{F} = O(1)$ and the buoyancy forcing is sufficiently strong that convective overturning motions are permitted. These motions feed back and adjust the mean stratification. Both systems of QGE filter out fast inertial-gravity waves on $o(L)$ scales but retain slow waves on scales larger than $O(L)$. The most pertinent geophysical application for the upright and tilted cases is to open-ocean deep convection (cf. ocean plumes in table 1). However, they are also relevant to laboratory experiments on rapidly rotating convection (Boubnov & Golitsyn 1990; Fernando, Chen & Boyer 1991; Maxworthy & Narimousa 1994; Ohlsen, Hart & Kittelman 1995; Liu & Ecke 1997; Sakai 1997; Hart & Ohlsen 1999; Levy & Fernando 2003) as well as recent direct numerical simulations of rapidly rotating convection (Julien *et al.* 1996*a, b*). The derivation of the upright version of these QGE is considerably simpler because only one vertical length scale is present. Indeed, the UNH-QGE II were originally derived by Julien *et al.* (1998*a*) for Rayleigh–Bénard convection rotating about the local vertical (i.e. for convection at the north pole), using the horizontal scale selected by linear stability theory, and generalized to the f -plane by Julien & Knobloch (1998). However, because of the use of Cartesian coordinates, the result in the latter case could only be written down in Fourier space. In §6.1.2 we show that closed equations for the f -plane can be obtained in differential form using non-orthogonal coordinates, and reconcile earlier derivations with the present derivation of UH-QGE and TH-QGE where linear theory is not invoked. The derivation confirms that the TNH-QGE II is the correct system of equations for capturing turbulent f -plane dynamics in this regime.

The system TNH-QGE III (table 4, equation (3.6)), derived in §6.2 for the parameter values given in table 3 (TNH-QGE III, row 6), captures the effects of spatial modulation in the \hat{y} -direction on scales $A_y \sim Ro^{-1}$. Near the tropics this system transitions to SNH-QGE III (figure 4). Such equations therefore capture the interaction between equatorial waves and convection, and as a result may have implications for phenomena such as the Madden–Julian oscillation (Madden & Julian 1972, 1994). They are also appropriate for the so-called ‘banana’ cell regime of convection in rapidly rotating shells (Busse 1970, 2002; Hart, Glatzmaier & Toomre 1986; Aurnou & Olson 2001). For $A_y = o(Ro^{-1})$, the β -effect becomes negligible and meridional modulation is no longer required (see (b) above and figure 4).

4. Small aspect ratio quasi-geostrophic regime

In this section, we use (2.25*a*)–(2.25*e*) to derive, in the Cartesian coordinate system \hat{x} , \hat{y} , \hat{z} , reduced systems of equations with balanced dynamics corresponding to upright geostrophy (table 2, row 1). Column 3, deduced from equation (2.26), shows that the

aspect ratio A_z required for geostrophy varies from unity ($A_z = 1$) to small ($A_z = o(1)$) as the colatitude increases from the pole ($\eta_3 \rightarrow 1, \eta_2 \rightarrow 0$) through the extratropical region ($\eta_3, \eta_2 = O(1)$). In fact, condition (2.26) indicates that in the polar region upright geostrophy occurs because η_2 is small; elsewhere we can obtain upright geostrophy by choosing a small aspect ratio ($A_z = o(1)$), and the required aspect ratio decreases with increasing colatitude. Despite this difference, both regimes lead to reduced QGE of identical form (UH-QGE; table 4, equation (3.1)), cf. figure 4.

To account for these differences in a unified manner we introduce the parameter $\delta := A_z \eta_2 = o(1)$ to be used as an asymptotic expansion parameter in addition to $\epsilon := Ro$. We thus set $\epsilon, \delta \ll 1$ and pose the double expansion

$$\mathbf{v} = \sum_{i,j} \epsilon^i \delta^j \mathbf{v}_{ij}. \quad (4.1)$$

In addition, following the criteria for upright geostrophy given in table 2 and the parameter magnitudes summarized in table 3 for UH-QGE, we choose the anisotropic spatial scales

$$A_y \equiv 1, \quad A_z \equiv \delta/\eta_2, \quad A_\beta = \epsilon\beta \quad (4.2)$$

and take

$$P = \epsilon^{-1}, \quad \Gamma = \frac{\eta_2}{\epsilon\delta}. \quad (4.3)$$

The source terms $\mathcal{S}_u, \mathcal{S}_b$ are taken to be $O(1)$. Under these conditions the buoyancy forcing as measured by Γ is sufficiently strong that the Taylor–Proudman constraint $\partial_z \mathbf{u}_{00} = 0$ is relaxed, and the geostrophic balance (2.31a) is replaced at $O(\epsilon^{-1})$ and $O(\eta_2 \epsilon^{-1} \delta^{-1})$ in (2.25a, b) and (2.25c) by

$$\eta_3 \widehat{\mathbf{z}} \times \mathbf{u}_{00} = -\nabla_\perp p_{00}, \quad (4.4a)$$

$$0 = -\partial_z p_{00} + b_{00}. \quad (4.4b)$$

These relations imply a horizontal geostrophic and a vertical hydrostatic balance, in addition to horizontal non-divergence

$$\nabla_\perp \cdot \mathbf{u}_{00} = 0. \quad (4.5)$$

From the continuity equation (2.25e) it now follows that $\partial_z w_{00} \equiv 0$ and hence impenetrable boundaries imply that $w_{00} = 0$ throughout the layer. The solution to these equations is given in table 4, equation (3.1a), with the ‘00’ subscript replaced by ‘0’. Higher asymptotic balances from equation (2.25c) are not considered since they are not required for the derivation of the reduced equations.

If $\epsilon = o(\delta)$ we must consider $O(\epsilon^{-1}\delta)$ terms in equations (2.25a, b). We obtain

$$\eta_3 \widehat{\mathbf{z}} \times \mathbf{u}_{01} = -\nabla_\perp p_{01} \quad (4.6)$$

and hence that

$$\nabla_\perp \cdot \mathbf{u}_{01} = 0. \quad (4.7)$$

From the continuity equation (2.25e) at $O(\delta)$ we find that $\partial_z w_{01} \equiv 0$ and impenetrable boundaries therefore imply that $w_{01} = 0$ as well. These results extend to $O(\epsilon^{-1}\delta^n)$ terms all of which can in principle be larger than $O(\epsilon^0)$ terms. Thus, $w_{0n} = 0, n > 0$. Finally, the momentum equations (2.25a) and (2.25b) at $O(\epsilon^0)$ and the continuity equation (2.25e) at $O(\epsilon)$ imply

$$D_t^{00} \mathbf{u}_{00\perp} + \eta_3 \widehat{\mathbf{z}} \times \mathbf{u}_{10\perp} + \eta_2 \beta y \widehat{\mathbf{z}} \times \mathbf{u}_{00\perp} = -\nabla_\perp p_{10} + \mathcal{S}_{\mathbf{u}_{00\perp}}, \quad (4.8a)$$

$$\nabla_\perp \cdot \mathbf{u}_{10\perp} + \partial_z w_{10} = 0, \quad (4.8b)$$

where $D_t^{00} = \partial_t + \mathbf{u}_{00} \cdot \nabla_{\perp}$. From equations (4.8) we obtain the vertical vorticity equation

$$D_t^{00} \omega_{00} - \eta_3 \partial_z w_{10} + \beta \eta_2 v_{00} = \widehat{\mathbf{z}} \cdot \nabla \times \mathcal{S}_{\mathbf{u}_{00\perp}}, \quad (4.9)$$

where $\omega_{00} \equiv \widehat{\mathbf{z}} \cdot \nabla \times \mathbf{u}_{00} = \nabla_{\perp}^2 \Psi_{00}(\mathbf{x}, t)$. It is clear that closure requires the determination of w_{10} in terms of the leading-order variables. Such a closure follows from the buoyancy equation (2.25d) if the stable background stratification is sufficiently strong. Specifically, when $\mathcal{F} = o(\epsilon^{1/2})$, asymptotic balance requires that we take $w_{10} = 0$. In this case, unless the source term $\mathcal{S}_{\mathbf{u}_{00\perp}}$ contains vertical derivatives, equation (4.9) decouples in z , and the leading-order flow takes the form of vertically uncoupled ‘pancakes’.[†] In contrast, if we take $\mathcal{F} = \epsilon^{1/2}$, the buoyancy equation at $O(\epsilon^0)$ implies that

$$D_t^{00} b_{00} - w_{10} \partial_z \bar{\rho}(z) = \mathcal{S}_{b_{00}}. \quad (4.10)$$

Thus, according to (4.10), a small vertical velocity drives buoyancy anomalies by extracting potential energy from the background stratification. Elimination of w_{10} and b_{00} using equation (3.1a) now leads to the forced UH-QGE (table 4, equations (3.1b) and (3.1c)) with the subscript ‘00’ replaced by ‘0’. In the polar regions identical equations hold, provided we choose $A_z = 1$ and $\Gamma = \epsilon^{-1}$. These equations can also be obtained by taking the formal limit $\eta_2 \rightarrow 0$, $\eta_3 \rightarrow 1$, with $\delta/\eta_2 \equiv A_z \rightarrow 1$. As a consequence the β -effect is negligible in this region.

In the absence of forcing, the potential vorticity q_0 (table 4, equation (3.1c)) is conserved along with all arbitrary functions $F(q_0)$ of q_0 . Also conserved are the Eulerian quantities $\langle b_{00} \rangle$ and the positive definite total energy

$$\begin{aligned} \langle E_{00} \rangle &\equiv -\frac{1}{2} \langle \Psi_{00} q_{00} \rangle = \frac{1}{V} \int d\mathbf{x}_{\perp} dz \frac{1}{2} \left(\mathbf{u}_{00\perp} \cdot \mathbf{u}_{00\perp} - \frac{1}{\partial_z \bar{\rho}(z)} b_{00}^2 \right) \\ &\equiv \frac{1}{V} \int d\mathbf{x}_{\perp} dz \frac{1}{2} \left(\nabla_{\perp} \Psi_{00} \cdot \nabla_{\perp} \Psi_{00} - \frac{\eta_3^2}{\partial_z \bar{\rho}(z)} \partial_z \Psi_{00} \partial_z \Psi_{00} \right), \end{aligned} \quad (4.11)$$

cf. equations (2.10) and (2.11). These combined properties are directly responsible for the $k^{-5/3}$ inverse energy cascade and the k^{-3} forward enstrophy cascade of QG dynamics (McWilliams, Weiss & Yavneh 1994; Vallis 1996; Salmon 1998; Smith & Waleffe 2002). In this connection we mention that our expression for the potential vorticity q_0 differs from that derived from the so-called ‘primitive’ equations by Vallis (1996) through the effects of the background stratification. However, the primitive equations assume that the flow is strictly hydrostatic, and Vallis focuses on the somewhat different regime $Fr \sim Ro A_z$.

5. Intermediate quasi-geostrophic regime

In this section, we use the Cartesian coordinates $\widehat{\mathbf{x}}, \widehat{\mathbf{y}}, \widehat{\mathbf{z}}$ to derive the TQH-QGE (table 4, equation (3.2)) valid for motions in the extratropical regions when $L \sim L_y \sim L_z$ (see figure 3). Since geostrophy prevails at all scales, a multiple scale approach is not required. The distinguished parameter values used in the asymptotic theory are given in table 3. Consistent with these parameters and the criteria for tilted geostrophy given in table 2, we choose isotropic spatial scales,

$$A_y \equiv 1, \quad A_z \equiv 1, \quad A_{\beta} = \epsilon \beta, \quad (5.1)$$

[†] This is true both for Rayleigh friction, and for classical diffusion in the extratropics where $A_z = o(1)$ and $\mathcal{S}_{\mathbf{u}_{00\perp}} = (1/Re) \nabla_{\perp}^2 \mathbf{u}_{00\perp}$. In the polar region $A_z \sim 1$ and coupling occurs through vertical diffusion: $\mathcal{S}_{\mathbf{u}_{00\perp}} = (1/Re) \nabla^2 \mathbf{u}_{00\perp}$.

and take

$$P = \epsilon^{-1}, \quad \Gamma = \epsilon^{-1}, \quad (5.2)$$

where $Ro \equiv \epsilon \ll 1$.

Under these conditions the leading-order balance is

$$\hat{\eta}_0 \times \mathbf{u}_0 = -\nabla p_0 + b_0 \hat{\mathbf{z}}. \quad (5.3)$$

Like its upright counterpart this relation implies a horizontal geostrophic balance. However, the thermal wind balance

$$\hat{\eta}_0 \cdot \nabla \mathbf{u}_0 = -\nabla \times b_0 \hat{\mathbf{z}} \quad (5.4)$$

now also holds, implying $w_0 = 0$. Departure from classical QG occurs in the vertical momentum balance which now leads to the quasi-hydrostatic balance

$$-\eta_2 u_0 = -\partial_z p_0 + b_0. \quad (5.5)$$

The solution to this leading-order tilted geostrophic balance is given in table 4, equation (3.2a). The reduced equations describing quasi-geostrophic motions are obtained at next order in perturbation theory. Specifically, at $O(\epsilon^0)$ in the momentum equation (2.25a) and $O(\epsilon)$ in the continuity equation (2.25d) we obtain

$$D_t^0 \mathbf{u}_{0\perp} + \hat{\eta}_0 \times \mathbf{u}_1 - \beta y \hat{\eta}_1 \times \mathbf{u}_{0\perp} = -\nabla p_1 + b_1 \hat{\mathbf{z}} + \mathcal{S}_{u_{0\perp}}, \quad (5.6a)$$

$$\nabla \cdot \mathbf{u}_1 = 0. \quad (5.6b)$$

Eliminating the pressure term from these equations leads to the vertical vorticity equation

$$D_t^0 \omega_0 - \hat{\eta}_0 \cdot \nabla w_1 + \beta \eta_2 v_0 = \hat{\mathbf{z}} \cdot \nabla \times \mathcal{S}_{u_{0\perp}}, \quad (5.7)$$

where $\omega_0 \equiv \hat{\mathbf{z}} \cdot \nabla \times \mathbf{u}_0 = \nabla_{\perp}^2 \Psi_0(\mathbf{x}, t)$.

Closure requires the determination of w_1 in terms of the leading-order variables. Such a closure follows from the buoyancy equation (2.25d) if the background stratification is sufficiently strong. When $\mathcal{F} = o(\epsilon^{1/2})$, we require that $w_1 = 0$, and any coupling in the vertical can only occur through $\mathcal{S}_{u_{0\perp}}$, for example, through classical diffusion. In contrast, when $\mathcal{F} = \epsilon^{1/2}$ fully three-dimensional spatial dynamics are captured, and the buoyancy equation at $O(\epsilon^0)$ implies

$$D_t^0 b_0 - w_1 \partial_z \bar{\rho}(z) = \mathcal{S}_{b_0}. \quad (5.8a)$$

Elimination of w_1 and b_0 from these equations leads to an equation that can be recast, after some manipulation, into the forced TQH-QGE (table 4, equation (3.2)) on the β -plane. This is the form of the quasi-geostrophic equation in the presence of slanted rotation, as derived by Embid & Majda (1998). Thus the traditional and slanted quasi-geostrophic equations are connected through the mapping $\hat{\mathbf{z}} \cdot \nabla \rightarrow \hat{\eta}_0 \cdot \nabla$; this mapping can be used to construct the conserved quantities for this system from those for UH-QGE discussed in §4 and in Appendix B. Of course, differences in boundary forcing between the two cases may be responsible for differences in the resulting evolution.

The scaling used in the above derivation was designed to retain the β -effect on the horizontal scale L , implicitly requiring that the layer be sufficiently deep. Under these conditions the effects of stratification and sphericity gain importance; these may be included within an anelastic formulation (Bannon 1996; Gough 1969), an approach not pursued here. On smaller scales for which the Boussinesq equations are valid the β -effect may drop out. When this is the case we obtain a two-dimensional

version of a system of reduced equations called TNH-QGE III in the extratropics, and SNH-QGE III in the tropics ($\widehat{\boldsymbol{\eta}}_0 = \widehat{\mathbf{y}}$) with $\partial_\gamma \equiv 0$ (see figure 4).

6. Large aspect ratio quasi-geostrophy regimes

In this section we derive the reduced equations for large aspect ratio motions characterized by $A_z \gg 1$ or $A_y \gg 1$. On the scale L such motions are constrained by the tilted geostrophic balance, requiring the introduction of a modulation scale X . Two distinct classes of reduced equations are identified, one associated with upright but tilted columns, where $X = Z$, and the other with sideways but upwardly tipped columns, where $X = Y$. In both classes strictly upright or sideways versions of the QGE can be obtained by taking appropriate limits: $\widehat{\boldsymbol{\eta}}_0 \rightarrow \widehat{\mathbf{z}}$ in the polar region for $X = Z$ and $\widehat{\boldsymbol{\eta}}_0 \rightarrow \widehat{\mathbf{y}}$ in the equatorial region for $X = Y$ (see figures 3 and 4). Throughout we make use of the fact that at leading order, the averaged system is in hydrostatic balance with vanishing mean flows, cf. §2.3.4.

6.1. Tilted columnar motions

The tilted quasi-hydrostatic QGE (TQH-QGE) extend to the columnar regime characterized by $A_z = o(\epsilon^{-1})$. We refer to the resulting reduced system as TH-QGE (table 4, equation (3.3); see figure 3). Once $A_z \sim \epsilon^{-1}$, non-hydrostatic motions become important, and couple to the geostrophically constrained dynamics. The reduced equations that result are referred to as TNH-QGE of types I and II and are distinguished by the strength of the background stratification (table 4, equations (3.4) and (3.5); see also figure 3). The parameter values used in the asymptotic development are given in table 3. In all cases the leading tilted geostrophic balance is given by

$$\widehat{\boldsymbol{\eta}}_0 \times \mathbf{u}'_0 = -\nabla p'_0, \quad (6.1)$$

together with the continuity condition

$$\nabla \cdot \mathbf{u}'_0 = 0. \quad (6.2)$$

The resulting solution obeys the Taylor–Proudman constraint $\partial_\eta \mathbf{u}'_0 = \partial_\eta p'_0 = 0$, and is given in table 4 in equations (3.3a), (3.4a) and (3.5a).

The associated QGE are most easily derived in a non-orthogonal coordinate system with covariant basis $(\mathbf{g}_1, \mathbf{g}_2, \mathbf{g}_3) \equiv (\widehat{\mathbf{x}}, \widehat{\mathbf{y}}, \widehat{\boldsymbol{\eta}}_0)$ described in Appendix A, case A. In these coordinates, the velocity and vorticity fields are given by

$$\mathbf{u}'_0 = -\frac{1}{\eta_3} \partial_{\widehat{\mathbf{y}}} \Psi_0 \widehat{\mathbf{x}} + \frac{1}{\eta_3} \partial_{\widehat{\mathbf{x}}} \Psi_0 \widehat{\mathbf{y}} + \left(\nabla_{\perp}^2 \Phi_0 - \frac{\eta_2}{\eta_3} \partial_{\widehat{\mathbf{x}}} \Psi_0 \right) \widehat{\boldsymbol{\eta}}_0, \quad (6.3a)$$

$$\boldsymbol{\omega}'_0 = \frac{1}{\eta_3} \nabla_{\perp}^2 \partial_{\widehat{\mathbf{y}}} \Phi_0 \widehat{\mathbf{x}} - \frac{1}{\eta_3} \nabla_{\perp}^2 \partial_{\widehat{\mathbf{x}}} \Phi_0 \widehat{\mathbf{y}} + \left(\nabla_{\perp}^2 \Psi_0 + \frac{\eta_2}{\eta_3} \nabla_{\perp}^2 \partial_{\widehat{\mathbf{x}}} \Phi_0 \right) \widehat{\boldsymbol{\eta}}_0, \quad (6.3b)$$

where $\nabla_{\perp}^2 = \partial_{\widehat{\mathbf{x}}}^2 + \eta_3^{-2} \partial_{\widehat{\mathbf{y}}}^2$ and we have set $\partial_\eta = 0$. In shorthand component form, we write these quantities as $\mathbf{u}'_0 = (\widetilde{u}'_0, \widetilde{v}'_0, \widetilde{w}'_0)$, $\boldsymbol{\omega}'_0 = (\widetilde{\omega}'_{01}, \widetilde{\omega}'_{02}, \widetilde{\omega}'_{03})$. Also useful for the purposes of vector operations is the dual basis \mathbf{g}^i satisfying $\mathbf{g}^i \cdot \mathbf{g}_j = \delta_j^i$. In Cartesian coordinates (x, y, z) these are given by $\mathbf{g}^1 = \widehat{\mathbf{x}}$, $\mathbf{g}^2 = \widehat{\mathbf{y}} - (\eta_2/\eta_3)\widehat{\mathbf{z}}$, $\mathbf{g}^3 = (1/\eta_3)\widehat{\mathbf{z}}$, and the unit rotation vector $\widehat{\boldsymbol{\eta}}_0 = \eta_2 \mathbf{g}^2 + \mathbf{g}^3$. Using the definition of the dot product given in Appendix A, case A, the velocity and vorticity components along the axis of rotation are $\widehat{\boldsymbol{\eta}}_0 \cdot \mathbf{u}'_0 = \nabla_{\perp}^2 \Phi_0$ and $\widehat{\boldsymbol{\eta}}_0 \cdot \boldsymbol{\omega}'_0 = \nabla_{\perp}^2 \Psi_0$, respectively. Thus motions perpendicular to $\widehat{\boldsymbol{\eta}}_0$ are entirely determined by Ψ_0 , and Ψ_0 represents the geostrophic streamfunction. In contrast, motions along the rotation axis are determined by the ageostrophic

streamfunction Φ_0 . The vertical velocity and vorticity components are given by $\hat{z} \cdot \mathbf{u}'_0 = \eta_3 \tilde{w}'_0$ and $\hat{z} \cdot \boldsymbol{\omega}'_0 = \eta_3 \tilde{\omega}'_{03}$, respectively.

6.1.1. TH-QGE

The first case we consider is TH-QGE. The criteria for tilted geostrophy (equation (6.1)) in table 2 and the parameter values given in table 3 lead to the following choice of anisotropic scales:

$$A_y = 1, \quad A_z = 1, \quad A_Y = \infty, \quad A_Z = o(\epsilon^{-1}), \quad A_T = \infty, \quad A_\beta = o(1). \quad (6.4)$$

Here, $Ro = \epsilon \ll 1$. As deduced in §2.3.4 we also take

$$P = \epsilon^{-1}, \quad \Gamma = \epsilon^{-1} A_Z^{-1}. \quad (6.5)$$

The derivation of the reduced equations requires a double asymptotic expansion of the form

$$\mathbf{v} = \sum_{i,j} \epsilon^i \delta^j \mathbf{v}_{ij}, \quad (6.6)$$

where $\delta = \epsilon A_Z \ll 1$.

At $O(\epsilon^{-1})$ in the fluctuating momentum equation (2.54a) we obtain the tilted geostrophic balance (6.1) for \mathbf{u}'_{00} and p'_{00} , while the continuity equation yields the balance

$$\nabla \cdot \mathbf{u}'_{00} = 0. \quad (6.7)$$

The solution of these equations is given in (3.3a), and in component form in (6.3). The continuity equation at $O(A_Z^{-1})$, $O(\delta)$ and $O(\epsilon)$ leads to the following balances as well:

$$\eta_3 \partial_Z \tilde{w}'_{00} = 0, \quad (6.8a)$$

$$\nabla \cdot \mathbf{u}'_{01} = 0, \quad (6.8b)$$

$$\nabla \cdot \mathbf{u}'_{10} + \eta_3 \partial_Z \tilde{w}'_{01} = 0. \quad (6.8c)$$

Thus in the presence of impenetrable boundaries $\tilde{w}'_{00} \equiv 0$ and vertical motions are weak. From equation (6.3a) we find that

$$\nabla_{\perp}^2 \Phi_{00} = \frac{\eta_2}{\eta_3} \partial_{\hat{x}} \Psi_{00}. \quad (6.9)$$

At $O(\delta^{-1})$ and $O(\epsilon^{-1}\delta)$ the momentum equation (2.54a) leads to hydrostatic and geostrophic balance:

$$\partial_Z p'_{00} - b'_{00} = 0, \quad (6.10a)$$

$$\hat{\eta}_0 \times \mathbf{u}'_{01} + \nabla p'_{01} = 0. \quad (6.10b)$$

Equations (6.1) and (6.10a) show that the leading-order variables \mathbf{u}'_{00} , p'_{00} and b'_{00} are completely determined by Ψ_{00} ; in particular $\partial_{\eta} b'_{00} = 0$ as well. In view of the continuity condition (6.8b), the solution to (6.10b) also obeys the Taylor–Proudman constraint $\partial_{\eta} \mathbf{u}'_{01} = \partial_{\eta} p'_{01} = 0$, and so has identical form to that given in (6.3). We remark that the asymptotic ordering of (6.8a), (6.8b) and (6.10a), (6.10b) conclusions $A_Z = o(\epsilon^{-1/2})$. When $A_Z > O(\epsilon^{-1/2})$ this ordering is reversed, but the essential results $\tilde{w}'_{00} = 0$ and $b'_{00} = \partial_Z \Psi_{00}$ are unchanged. In the special case $A_Z = \epsilon^{-1/2}$, equations (6.8a), (6.8b) and

(6.10a), (6.10b) arise at the same order and so are combined. In this case an expansion in the single parameter $\epsilon^{1/2}$ suffices, and leads to identical leading-order results.†

When $\delta^n/\epsilon \gg 1$, all corrections \mathbf{u}'_{0n} are in geostrophic balance with the corresponding pressure gradient $\nabla p'_{0n}$, and $\tilde{w}'_{0n} = 0$. Thus the next non-trivial contribution arises at $O(\epsilon^0)$:

$$\hat{\eta}_0 \times \mathbf{u}'_{10} + \nabla p'_{10} = -D_t^{00} \mathbf{u}'_{00} - (\partial_Z p'_{01} - b'_{01}) \hat{\mathbf{z}} + \mathcal{S} \mathbf{u}'_{00}, \quad (6.11)$$

where $D_t^{00} = \partial_t + \mathbf{u}'_{00\perp} \cdot \nabla_\perp$ and $\mathbf{u}'_{00\perp} \cdot \nabla_\perp f = \frac{1}{\eta_3} J[\Psi_{00}, f]$; here $J[\Psi_{00}, f] := \partial_{\bar{x}} \Psi_{00} \partial_{\bar{y}} f - \partial_{\bar{y}} \Psi_{00} \partial_{\bar{x}} f$ is the Jacobian. An identical result holds for the case $A_Z = \epsilon^{-1/2}$. Applying $\nabla \times$ and using (6.8c) gives

$$-\hat{\eta}_0 \cdot \nabla \mathbf{u}'_{10} = -D_t^{00} \boldsymbol{\omega}'_{00} + \boldsymbol{\omega}'_{00} \cdot \nabla \mathbf{u}'_{00} + \hat{\eta}_0 \eta_3 \partial_Z \tilde{w}'_{01} - \nabla \times (\partial_Z p'_{01} - b'_{01}) \hat{\mathbf{z}} + \nabla \times \mathcal{S} \mathbf{u}'_{00}. \quad (6.12)$$

This equation can be viewed as a differential equation for \mathbf{u}'_{10} . For a solution to exist we must impose the solvability condition obtained upon averaging the equation over η . We obtain

$$D_t^{00} \boldsymbol{\omega}'_{00} - \boldsymbol{\omega}'_{00} \cdot \nabla \mathbf{u}'_{00} - \hat{\eta}_0 \eta_3 \partial_Z \tilde{w}'_{01} = -\nabla \times (\partial_Z p'_{01} - \langle b'_{01} \rangle_\eta) \hat{\mathbf{z}} + \nabla \times \mathcal{S} \mathbf{u}'_{00}, \quad (6.13)$$

where

$$\langle b'_{01} \rangle_\eta \equiv \lim_{L_\eta \rightarrow \infty} \frac{1}{L_\eta} \int_{L_\eta} b'_{01} d\eta. \quad (6.14)$$

We find below that \tilde{w}'_{01} can be related to Ψ_{00} through the buoyancy equation for b'_{00} . To eliminate the contribution from the unknown quantities p'_{01} and b'_{01} we take $\hat{\mathbf{z}} \cdot$ of (6.13). To perform this operation in non-orthogonal coordinates we use the dual space representation $\hat{\mathbf{z}} = \eta_3 \mathbf{g}_3$ and use (6.3b) and the result (6.9) to obtain

$$\hat{\mathbf{z}} \cdot \boldsymbol{\omega}'_{00} = \eta_3 \nabla_\perp^2 \Psi_{00} + \eta_2 \nabla_\perp^2 \partial_{\bar{x}} \Phi_{00} = \frac{1}{\eta_3} (\partial_{\bar{x}}^2 + \partial_{\bar{y}}^2) \Psi_{00} := \frac{1}{\eta_3} \widehat{\nabla}_\perp^2 \Psi_{00}, \quad (6.15a)$$

$$\hat{\mathbf{z}} \cdot \mathbf{u}'_{00} \equiv \eta_3 \tilde{w}'_{00} = 0. \quad (6.15b)$$

Equation (6.13) then becomes

$$D_t^{00} \widehat{\nabla}_\perp^2 \Psi_{00} - \eta_3^3 \partial_Z \tilde{w}'_{01} = \eta_3 \hat{\mathbf{z}} \cdot \nabla \times \mathcal{S} \mathbf{u}'_{00}. \quad (6.16)$$

Closure requires the determination of \tilde{w}'_{01} in terms of the leading-order variables. Such a closure follows from the buoyancy equation

$$D_t^{00} b'_{00} - \frac{\epsilon}{\mathcal{F}^2} \eta_3 \tilde{w}'_{01} \partial_Z \bar{\rho}(Z) = \mathcal{S} b'_{00}. \quad (6.17)$$

When $\mathcal{F} = o(\epsilon^{1/2})$ an asymptotic balance requires that we take $\tilde{w}'_{01} = 0$. In this case unless the source term $\mathcal{S} \mathbf{u}'_{00\perp}$ contains vertical derivatives, equation (6.16) decouples in Z . In contrast, when $\mathcal{F} = \epsilon^{1/2}$ the buoyancy equation couples to equation (6.16) through \tilde{w}'_{01} , and fully three-dimensional spatial dynamics result. Equations (6.16)–(6.17) then collapse to the reduced system TH-QGE summarized in table 4, equation (3.3). This system is valid in the entire range $1 < A_Z < \epsilon^{-1}$. However, for weaker stratification, $\mathcal{F} > O(\epsilon^{1/2})$, no closure is obtained, and a reduction to a reduced system does not appear possible.

† To show this we apply $\hat{\eta}_0 \cdot$ and $\hat{\eta}_0 \cdot \nabla \times$ to the combined equations (6.10a), (6.10b), $\hat{\eta}_0 \times \mathbf{u}'_{01} + \nabla p'_{01} = (\partial_Z p'_{00} - b'_{00}) \hat{\mathbf{z}}$, average over η , and use the combined continuity equations (6.8a), (6.8b), $\nabla \cdot \mathbf{u}'_{01} + \eta_3 \partial_Z \tilde{w}'_{00} = 0$. Here the subscript ‘01’ is associated with terms of order $\epsilon^{1/2}$.

The system TH-QGE (table 4, equations (3.3*b*) and (3.3*c*)) is functionally identical to classical UH-QGE (table 4, equations (3.1*b*) and (3.1*c*)). With the caveat that differences may exist between boundary forcings, it follows that there is an one–one mapping ($\eta_3 y \rightarrow y$) between TH-QGE and UH-QGE. In the polar region this isomorphism is trivial. It follows that the system TH-QGE possesses all of the characteristic dynamics found for the classical UH-QGE (McWilliams *et al.* 1994, 1999), including an inverse energy cascade and free evolution to columns of oppositely signed potential vorticity. However, in the extratropics TH-QGE is valid only in the non-orthogonal coordinate system $(\hat{x}, \hat{y}, \hat{\eta}_0)$ with coordinate variables \tilde{x}, \tilde{y}, Z .

In the absence of forcing, the system TH-QGE conserves the potential vorticity q_{00} (table 4, equation (3.3*c*)) and its functionals $F(q_{00})$. Likewise, the energy $\langle E_{00} \rangle = -\frac{1}{2} \langle \Psi_{00} q_{00} \rangle$ is also conserved.

6.1.2. TNH-QGE

We consider next the derivation of the reduced system TNH-QGE describing tilted non-hydrostatic motions when $L_z \gg L$, in the case where $A_z = O(\epsilon^{-1})$ and vertical motions become comparable with horizontal motions. We consider two cases, depending on the magnitude of the Froude number \mathcal{F} . The criteria for tilted geostrophy (equation (6.1)) are given in table 2.

Type I

Table 3 indicates that the appropriate parameter values for TNH-QGE I are

$$A_y = 1, \quad A_z = 1, \quad A_Y = \infty, \quad A_Z = \epsilon^{-1}, \quad A_T = \infty, \quad A_\beta = o(1) \quad (6.18)$$

and

$$P = \epsilon^{-1}, \quad \Gamma = 1, \quad (6.19)$$

where $Ro = \epsilon \ll 1$. The tilted geostrophic balance (6.1) now follows from (2.54*a*) and (2.54*c*) at leading order; the solution of these equations is given in (3.4*a*) and in component form in (6.3).

A closed system of quasi-geostrophic equations in non-orthogonal coordinates is obtained from the fluctuating momentum and buoyancy equations (2.54*a*) and (2.54*b*) at $O(\epsilon^0)$ and the continuity equation (2.54*c*) at $O(\epsilon)$:

$$\hat{\eta}_0 \times \mathbf{u}'_1 + \nabla p'_1 = -D_t^0 \mathbf{u}'_0 - (\partial_z p'_0 - b'_0) \hat{\mathbf{z}} + \mathcal{S}_{u'_0}, \quad (6.20a)$$

$$D_t^0 b'_0 - \frac{\epsilon}{\mathcal{F}^2} \eta_3 \tilde{w}'_0 \partial_z \bar{\rho}(Z) = \mathcal{S}_{b'_0}, \quad (6.20b)$$

$$\nabla \cdot \mathbf{u}'_1 + \eta_3 \partial_z \tilde{w}'_0 = 0. \quad (6.20c)$$

Equations (6.20*a*) and (6.20*c*) can be viewed as differential equations for \mathbf{u}'_1 and p'_1 . To impose the required solvability condition we apply the operations $\hat{\eta}_0 \cdot$ and $\nabla \times$ to equation (6.20*a*), and obtain

$$\hat{\eta}_0 \cdot \nabla p'_1 = -\hat{\eta}_0 \cdot (D_t^0 \mathbf{u}'_0 + (\partial_z p'_0 - b'_0) \hat{\mathbf{z}} - \mathcal{S}_{u'_0}), \quad (6.21a)$$

$$-\hat{\eta}_0 \cdot \nabla \mathbf{u}'_1 = -D_t^0 \boldsymbol{\omega}'_0 + \boldsymbol{\omega}'_0 \cdot \nabla_{\perp} \mathbf{u}'_0 + \eta_3 \hat{\eta}_0 \partial_z \tilde{w}'_0 - \nabla \times (\partial_z p'_0 - b'_0) \hat{\mathbf{z}} + \nabla \times \mathcal{S}_{u'_0}. \quad (6.21b)$$

In addition, on applying $\hat{\eta}_0 \cdot \nabla$ to equation (6.20*b*) we obtain an advection–diffusion equation for $(\hat{\eta}_0 \cdot \nabla) b'_0$; it follows that

$$(\hat{\eta}_0 \cdot \nabla) b'_0 = 0. \quad (6.22)$$

Thus all leading-order variables are independent of η . Averaging equations (6.21a) and (6.21b) over η now yields the required reduced equations

$$D_t^0 \mathbf{u}'_0 = -(\partial_Z p'_0 - b'_0) \hat{\mathbf{z}} + \mathcal{S} u'_0, \quad (6.23a)$$

$$D_t^0 \omega'_0 - \omega'_0 \cdot \nabla_{\perp} \mathbf{u}'_0 - \eta_3 \hat{\eta}_0 \partial_Z \tilde{w}'_0 = -\nabla \times (\partial_Z p'_0 - b'_0) \hat{\mathbf{z}} + \nabla \times \mathcal{S} u'_0. \quad (6.23b)$$

On taking $\hat{\eta}_0 \cdot$ of these equations and using the vector relations summarized in Appendix A we obtain the reduced equations for the streamfunctions Ψ_0 and Φ_0 listed in TNH-QGE I (table 4, equations (3.4b) and (3.4c)). Both are buoyantly forced, the former by zonal gradients in the anomaly b'_0 , the latter by b'_0 itself.

From the buoyancy equation (6.20b) we see that $\tilde{w}'_0 = 0$ (i.e. $\nabla_{\perp}^2 \Phi_0 = (\eta_2/\eta_3) \partial_Z \Psi_0$) whenever $\mathcal{F} = o(\epsilon^{1/2})$, and non-hydrostatic vertical motions are then of higher order. Equations (6.23a) and (6.23b) now show that $b'_0 = \partial_Z \Psi_0$ and that

$$D_t^0 \widehat{\nabla}^2 \Psi_0 = \eta_3 \hat{\mathbf{z}} \cdot \nabla \times \mathcal{S} u'_0. \quad (6.24)$$

This set of results is virtually identical to the system TH-QGE (table 4, equations (3.3b) and (3.3c)) with the exception that the vertical motions are too weak to extract potential energy from stretching in Z due to the Coriolis force. In contrast, when $\mathcal{F} = \epsilon^{1/2}$, fully three-dimensional motions result from the coupling with the buoyancy equation. The full system of reduced equations that results in the latter case, TNH-QGE I, is listed in table 4, equation (3.4). Finally, if $\mathcal{F} > O(\epsilon^{1/2})$, the coupling to the mean stratification $\bar{\rho}(Z)$ is suppressed, and buoyancy fluctuations b'_0 satisfy an advection–diffusion equation with no forcing terms and thus decay. Thus $O(1)$ buoyancy fluctuations are not permitted for these weaker stratifications when $\Gamma = 1$. This observation prompts an investigation into case II below where $\Gamma = \epsilon^{-1}$.

On assuming a constant background stratification $S := -\partial_Z \bar{\rho}(Z)$ in TNH-QGE I, the dispersion relation for (inviscid) plane inertial-gravity waves of the form $\exp[i(k_{\tilde{x}} \tilde{x} + k_{\tilde{y}} \tilde{y} + k_Z Z - \sigma t)]$ is given by

$$\sigma^2 = 0 \quad \text{or} \quad \sigma^2 = \frac{\eta_3^2 k_Z^2 + S(k_{\tilde{x}}^2 + k_{\tilde{y}}^2)}{k_{\tilde{x}}^2 + (1/\eta_3^2) k_{\tilde{y}}^2}. \quad (6.25)$$

The first relation identifies the slow vortical modes present in all the hydrostatic QGE derived thus far. The latter relation identifies planar inertial-gravity waves, on scales greater than $O(L)$, that are now permitted by the inclusion of non-hydrostatic effects, and agrees with the corresponding limit of the exact dispersion relation obtained from the full Boussinesq equations for three-dimensional non-hydrostatic oscillations. The individual contributions of rotation and stratification are clearly identifiable.

The nonlinear interaction between these modes is of considerable interest. Smith & Waleffe (2002) investigated such an interaction in the full Boussinesq equations in the regime $1/2 < N_0/f < \infty$, but not in the regime $N_0/f \rightarrow 0$ in which our reduced equations provide a simplified description of this phenomenon.

For TNH-QGE I, conservation of potential vorticity takes the form

$$D_t^0 q_0 = 0, \quad q_0 = \tilde{\omega}'_{03} - (\omega'_0 \cdot \nabla + \hat{\eta}_0 \cdot \hat{\mathbf{z}} \partial_Z) \left(\frac{b'_0}{\partial_Z \bar{\rho}} \right). \quad (6.26)$$

This expression for q_0 is remarkably similar to that characteristic of the hydrostatic quasi-geostrophic regime, and is most easily obtained from an asymptotic expansion of the general expression for the potential vorticity as discussed in Appendix B; its conservation can be demonstrated by direct, albeit lengthy, computation. Also

conserved by equation (3.4) are the quantities $\langle b'_0 \rangle$ and

$$\langle E_0 \rangle = \frac{1}{V} \int dx dZ \frac{1}{2} \left(\mathbf{u}'_0 \cdot \mathbf{u}'_0 - \frac{b_0'^2}{\partial_Z \bar{\rho}(Z)} \right). \quad (6.27)$$

Type II

As established above, the system TNH-QGE I cannot support $O(1)$ buoyancy fluctuations when the Froude number is insufficiently small, $\mathcal{F} > O(\epsilon^{1/2})$, and $\Gamma = 1$. In this section we derive the reduced system TNH-QGE II (table 4, equation (3.5)) that arises in this situation but for $\Gamma = \epsilon^{-1}$, where $Ro = \epsilon \ll 1$. As before, we select the scales

$$A_y = 1, \quad A_z = 1, \quad A_Y = \infty, \quad A_Z = \epsilon^{-1}, \quad A_\beta = o(1), \quad (6.28)$$

but now take

$$P = \epsilon^{-2}, \quad \Gamma = \epsilon^{-1} \quad (6.29)$$

and include the slow time scale T by taking $A_T = \epsilon^{-2}$. At $O(\epsilon^{-2})$, the fluctuating momentum equation (2.54a) implies that

$$\nabla p'_0 \equiv 0 \quad (6.30)$$

and hence that $p'_0 \equiv 0$. Likewise, when $\mathcal{F} \gg \epsilon^{1/2}$, the fluctuating buoyancy equation yields at leading order an advection–diffusion equation for b'_0 , implying that $b'_0 \equiv 0$. From the fluctuating momentum and continuity equations, it now follows that at leading order

$$\hat{\eta}_0 \times \mathbf{u}'_0 + \nabla p'_1 = 0, \quad \nabla \cdot \mathbf{u}'_0 = 0, \quad (6.31)$$

and hence that the leading-order problem again satisfies the Taylor–Proudman constraint $\partial_\eta \mathbf{u}'_0 = \partial_\eta p_1 = 0$. The corresponding solution is given in table 4, equation (3.5a), or in component form in equation (6.3); moreover $p'_1 = \Psi_0$.

At $O(\epsilon^0)$, the fluctuating momentum equation (2.54a) and at $O(\epsilon)$ the buoyancy and continuity equations (2.54b) and (2.54c) yield

$$\hat{\eta}_0 \times \mathbf{u}'_1 + \nabla p'_2 = -D_t^0 \mathbf{u}'_0 - (\partial_Z p'_1 - b'_1) \hat{\mathbf{z}} + \mathcal{S} u'_0, \quad (6.32a)$$

$$D_t^0 b'_1 + \eta_3 \tilde{w}'_0 \partial_Z (\bar{b}_0 - \mathcal{F}^{-2} \bar{\rho}(Z)) = \mathcal{S} b'_1, \quad (6.32b)$$

$$\nabla \cdot \mathbf{u}'_1 + \eta_3 \partial_Z \tilde{w}'_0 = 0. \quad (6.32c)$$

The solvability conditions for equation (6.32a) are identical to those obtained for Type I above, and lead to prognostic equations for the streamfunctions Ψ_0 and Φ_0 given in table 4, equations (3.5b) and (3.5c). Once again if $\mathcal{F} = o(1)$ then $\tilde{w}'_0 = 0$ and the leading-order motions are again hydrostatic with $b'_1 = \partial_Z \Psi_0$. However, when $\mathcal{F} = O(1)$, coupling is achieved through the buoyancy equation (6.32b), although $\partial_\eta b'_1 = 0$ continues to hold.

The resulting system requires an equation for \bar{b}_0 for closure. Such an equation is obtained from the mean buoyancy equation (2.53b) at $O(\epsilon^0)$,

$$\partial_T \bar{b}_0 + \partial_Z ((\eta_3 \nabla_\perp^2 \Phi_0 - \eta_2 \partial_x \Psi_0) b'_1) = \epsilon^{-2} \overline{\mathcal{S} b_0}, \quad (6.33)$$

and results in the closed set of reduced equations labelled TNH-QGE II (table 4, equation (3.5)). For classical diffusion $\epsilon^{-2} \overline{\mathcal{S} b_0} = P e^{-1} \partial_Z^2 \bar{b}_0$.

The linear dispersion relation obtained from the resulting system is identical to equation (6.25) except that the stratification parameter is now $S := \partial_Z (\bar{b}_0 - \bar{\rho}(Z))$. Thus, slow vortical modes and inertial-gravity waves are again present. Moreover,

in the presence of an unstable stratification, small-scale perturbations with sufficient magnitude to overcome diffusive effects can undergo a convective instability. The subsequent evolution of such perturbations is also described by the system TNH-QGE II. Inspection of these equations shows that buoyancy anomalies are driven by the extraction of potential energy from the mean stratification profile, (3.5c), while fluid motions are driven by departures from a vertical hydrostatic balance on small scales by the Coriolis forcing induced by ageostrophic motions involving the Z stretching term in equation (3.5b). The mean equation (6.33) describes the nonlinear feedback between these motions and the stratification profile: the vertical buoyancy flux modifies the stratification on the slow time scale $T = \epsilon^2 t$. An extensive numerical investigation of TNH-QGE II has recently been performed for the case of rotating Rayleigh–Bénard convection (Sprague *et al.* 2006).

For TNH-QGE II, conservation of potential vorticity takes the form

$$D_t^0 q_0 = 0, \quad q_0 = \omega'_{03} + (\omega'_0 \cdot \nabla + \hat{\eta} \cdot \hat{z} \partial_z) \left(\frac{b'_1}{\partial_z(\bar{b}_0 - \mathcal{F}^{-2}\bar{\rho})} \right). \quad (6.34)$$

Also conserved by equation (3.5) are the quantities $\langle b'_1 \rangle$ and

$$\langle E_0 \rangle = \frac{1}{V} \int d\mathbf{x} dZ \frac{1}{2} \left(\mathbf{u}'_0 \cdot \mathbf{u}'_0 + \frac{b_1'^2}{\partial_z(\bar{b}_0 - \mathcal{F}^{-2}\bar{\rho})} \right). \quad (6.35)$$

This conservation law is a consequence of case (iv) of §2.1.

6.2. Sideways columnar motions

The sideways non-hydrostatic (SNH) QGE describe flows in the tropics where sideways geostrophy describes the balanced dynamics (see table 2). These equations extend to the system TNH-QGE III representing similar dynamics in the extratropical region, i.e. in the regime where the vertical component of the rotation vector is also significant (see figure 3). The appropriate parameter regimes permitting such reduced dynamics are summarized in table 3. The main difference between the derivation of TNH-QGE I and II comes from the inclusion of the β -effect requiring the introduction of a slow scale Y . Consequently, the resulting reduced equations are most easily derived in the non-orthogonal coordinate system with covariant basis $(\mathbf{g}_1, \mathbf{g}_2, \mathbf{g}_3) \equiv (\hat{\mathbf{x}}, \hat{\eta}_0, \hat{\mathbf{z}})$ (see Appendix A, case B).

The leading tilted geostrophic balance is identified by equation (2.43a) in §2.3.3. However, the solution of the equations under the Taylor–Proudman constraint (2.44) is now given in table 4, equation (3.6a). In component form (see Appendix A, case B) the velocity and vorticity fields are given by

$$\mathbf{u}'_0 = \frac{1}{\eta_2} \partial_z \Psi_0 \hat{\mathbf{x}} + \left(\nabla_{\perp}^2 \Phi_0 + \frac{\eta_3}{\eta_2} \partial_{\hat{x}} \Psi_0 \right) \hat{\eta}_0 - \frac{1}{\eta_2} \partial_{\hat{x}} \Psi_0 \hat{\mathbf{z}}, \quad (6.36a)$$

$$\boldsymbol{\omega}'_0 = -\frac{1}{\eta_2} \nabla_{\perp}^2 \partial_z \Phi_0 \hat{\mathbf{x}} + \left(\nabla_{\perp}^2 \Psi_0 - \frac{\eta_3}{\eta_2} \nabla_{\perp}^2 \partial_{\hat{x}} \Phi_0 \right) \hat{\eta}_0 + \frac{1}{\eta_2} \nabla_{\perp}^2 \partial_{\hat{x}} \Phi_0 \hat{\mathbf{z}}, \quad (6.36b)$$

where $\nabla_{\perp}^2 = \partial_{\hat{x}}^2 + \eta_2^{-2} \partial_{\hat{z}}^2$ and $p'_0 = \Psi_0$ is the geostrophic streamfunction. Note that the geostrophic streamfunction permits non-hydrostatic motions in the vertical. For the purpose of performing vector operations, we note the dual basis $\mathbf{g}^1 = \hat{\mathbf{x}}$, $\mathbf{g}^2 = (1/\eta_2) \hat{\mathbf{y}}$, $\mathbf{g}^3 = -(\eta_3/\eta_2) \hat{\mathbf{y}} + \hat{\mathbf{z}}$, and the unit rotation vector $\hat{\eta}_0 = \mathbf{g}^2 + \eta_3 \mathbf{g}^3$. Using the definition of the dot product given in Appendix A, case B, the velocity and vorticity components along the axis of rotation are $\hat{\eta}_0 \cdot \mathbf{u}'_0 = \nabla_{\perp}^2 \Phi_0$ and $\hat{\eta}_0 \cdot \boldsymbol{\omega}'_0 = \nabla_{\perp}^2 \Psi_0$, respectively, while motions perpendicular to $\hat{\eta}_0$ are entirely determined by Ψ_0 . In

the meridional direction $\hat{\mathbf{y}}$, the velocity and vorticity are given by $\hat{\mathbf{y}} \cdot \mathbf{u}'_0 = \eta_2 \tilde{v}'_0$ and $\hat{\mathbf{y}} \cdot \boldsymbol{\omega}'_0 = \eta_2 \tilde{\omega}'_{02}$, respectively.

6.2.1. TNH-QGE III

As indicated in table 2 and table 3, row 6, we take $Ro \equiv \epsilon \ll 1$ and choose without loss of generality the anisotropic spatial scales

$$A_y = 1, \quad A_z = 1, \quad A_Y = \epsilon^{-1}, \quad A_Z = \infty, \quad A_T = \infty, \quad A_\beta = \epsilon^{-2} \beta \quad (6.37)$$

together with

$$P = \epsilon^{-1}, \quad \Gamma = 1. \quad (6.38)$$

At leading order the fluctuating momentum and continuity equations (2.54a) and (2.54c) yield the tilted geostrophic balance (6.1); the corresponding solution is given in equation (3.6a) and in component form in equation (6.36).

The corresponding system of quasi-geostrophic equations in primitive variables can be deduced at $O(\epsilon^0)$ in the fluctuating momentum equation and $O(\epsilon)$ in the buoyancy and continuity equations (2.54b) and (2.54c):

$$\hat{\boldsymbol{\eta}}_0 \times \mathbf{u}'_1 + \nabla p'_1 = -D_t^0 \mathbf{u}'_0 + \beta Y \hat{\boldsymbol{\eta}}_1 \times \mathbf{u}'_0 - \partial_Y p'_0 \hat{\mathbf{y}} + b'_0 \hat{\mathbf{z}} + \mathcal{S} u'_0, \quad (6.39a)$$

$$D_t^0 \left(b'_0 - \frac{1}{\mathcal{F}^2} \rho(z) \right) = \mathcal{S} b'_0, \quad (6.39b)$$

$$\nabla \cdot \mathbf{u}'_1 + \eta_2 \partial_Y \tilde{v}'_0 = 0. \quad (6.39c)$$

For a closed system we require that $\mathcal{F} = O(1)$. On applying $\hat{\boldsymbol{\eta}}_0 \cdot \nabla$ to equation (6.39b), we also deduce that

$$(\hat{\boldsymbol{\eta}}_0 \cdot \nabla) b'_0 = 0. \quad (6.40)$$

The operations $\hat{\boldsymbol{\eta}}_0 \cdot$ and $\nabla \times$ applied to equation (6.39a) now yield

$$\hat{\boldsymbol{\eta}}_0 \cdot \nabla p'_1 = \hat{\boldsymbol{\eta}}_0 \cdot \left(-D_t^0 \mathbf{u}'_0 + \beta Y \hat{\boldsymbol{\eta}}_1 \times \mathbf{u}'_0 - \partial_Y p'_0 \hat{\mathbf{y}} + b'_0 \hat{\mathbf{z}} + \mathcal{S} u'_0 \right), \quad (6.41a)$$

$$\hat{\boldsymbol{\eta}}_0 \cdot \nabla \mathbf{u}'_1 = D_t^0 \boldsymbol{\omega}'_0 - \boldsymbol{\omega}'_0 \cdot \nabla_{\perp} \mathbf{u}'_0 - \eta_2 \hat{\boldsymbol{\eta}}_0 \partial_Y \tilde{v}'_0 - \nabla \times (\beta Y \hat{\boldsymbol{\eta}}_1 \times \mathbf{u}'_0 - \partial_Y p'_0 \hat{\mathbf{y}} + b'_0 \hat{\mathbf{z}} + \mathcal{S} u'_0). \quad (6.41b)$$

The solvability conditions for these equations, obtained by averaging over η , require that the right-hand sides vanish. Projecting the latter onto $\hat{\boldsymbol{\eta}}_0$ results in a closed system, summarized in the streamfunction formulation in table 4, equation (3.6). In the limit $\hat{\boldsymbol{\eta}}_0 \rightarrow \hat{\mathbf{y}}$, this system becomes the system known as SNH-QGE III.

The quasi-geostrophic system TNH-QGE III (table 4, equation (3.6)) retains slow inertial-gravity waves on $O(L)$ scales or larger. In the case of constant background stratification $S := -\bar{\rho}(\tilde{z})/\mathcal{F}^2$ at the equator ($\hat{\boldsymbol{\eta}}_0 = \hat{\mathbf{y}}$, $\beta = 0$), the dispersion relation for such waves is

$$\sigma = 0, \quad \sigma^2 = \frac{k_Y^2 + k_{\tilde{x}}^2 S}{k_{\tilde{x}}^2 + k_{\tilde{z}}^2}, \quad (6.42)$$

assuming disturbances of the form $\exp[i(k_{\tilde{x}} \tilde{x} + k_Y Y + k_{\tilde{z}} \tilde{z} - \sigma t)]$. The first mode corresponds to meridional displacements along local equipotentials, i.e. to modes with $\tilde{u}'_0 = \tilde{w}'_0 \equiv 0$. The latter agrees with the corresponding limit of the exact dispersion relation for three-dimensional non-hydrostatic oscillations. Once again the individual contributions of rotation and stratification are clearly identifiable. Equatorial Rossby waves are described by a generalization of this dispersion relation that incorporates the β -effect, and requires the solution of an eigenvalue problem.

The system TNH-QGE III also conserves the potential vorticity

$$q_0 = \left(\left(\eta_2 \partial_Y + \beta \frac{Y}{\eta_2} \partial_z \right) + \boldsymbol{\omega}'_0 \cdot \nabla_\perp \right) (b'_0 - \mathcal{F}^{-2} \bar{\rho}(\bar{z})), \quad (6.43)$$

(see Appendix B) as can be verified by direct computation. In addition, $\langle b_0 \rangle$ and, for a linear density profile $\rho(z) = \alpha z$,

$$\langle E_0 \rangle = \frac{1}{V} \int d\tilde{\mathbf{x}} dY \frac{1}{2} \left(|\mathbf{u}'_0|^2 + v_0'^2 - \frac{b_0'^2}{\alpha} \right), \quad (6.44)$$

are both conserved. Here, since $\Gamma Fr = O(1)$ with $w'_0 \neq 0$, $b'_0 \neq 0$, energy is not conserved for general stratification, cf. case (iii) of §2.1.

TNH-QGE III and SNH-QGE III describe the dynamics on large meridional scales but zonal scales that are comparable to the layer depth. Anisotropic scaling of this type is most appropriate in the so-called ‘banana’ cell regime of convection in rapidly rotating shells. In this regime convection takes the form of a belt of Taylor–Proudman columns that precess around the rotation axis; such columns automatically have $A_z \sim 1$, and are modulated on a large meridional scale by the spherical geometry of the system (Busse 1970, 2002; Hart *et al.* 1986; Aurnou & Olson 2001). In contrast Majda & Klein (2003) focus on small meridional scales, while permitting the presence of large zonal scales; this assumption can also lead to a closed set of reduced equations.

7. Conclusions

According to classical texts (Pedlosky 1979; Gill 1982) the assumption of geostrophy involves an instantaneous relation between Coriolis wind and pressure, and is a consequence of neglecting inertial accelerations. Quasi-geostrophy is the dynamical theory which follows from the resolution of the degeneracy of geostrophy with the leading-order divergence condition. In this paper we have explored the possibility that the familiar quasi-geostrophic equations governing the behaviour of planetary-scale motions at mid-latitudes may be generalized to capture other regimes of interest to geophysical fluid dynamics. In order to do this we have systematically explored, as a function of the colatitude ϑ_0 , different length scales in the horizontal and vertical, together with a parallel exploration of the space of Froude numbers (measuring the strength of the ambient density stratification) and buoyancy numbers (measuring the strength of buoyancy forcing), all while assuming the motions are rotation-dominated, i.e. that the Rossby number is small. We have classified the resulting reduced QG models in terms of U-Upright, S-Sideways, or T-Tilted geostrophy, depending on whether the Coriolis force is dominated by the local vertical, horizontal, or both components of the rotation vector. The existence of these regimes determines bounds on all dimensionless parameters except for the Froude number Fr , which can be varied as part of the search for a closed reduced description of the geostrophically balanced leading-order flow. In cases where geostrophy does not prevail on all scales of interest, we have seen that a multiple-scale approach is required. Such regimes are described in terms of tilted geostrophy, with large-scale spatial modulation due to the stratification scale or the scale of the β -effect. By a judicious choice of these parameters within each geostrophic regime, we were able to locate regimes in which the balance equations that occur order by order in an asymptotic expansion close at a low order, but non-trivial vertical dependence is retained. This procedure resulted in a secondary

classification according to whether the resulting QGE describe H-hydrostatic, QH-quasi-hydrostatic or NH-non-hydrostatic motions. The resulting equations represent a reduced description in that they filter out inertial-gravity waves on scales L and smaller, and in the extratropics describe the dynamics in the bulk of the layer, outside of any boundary layers introduced through dissipation. In particular, when $A_z \equiv L_z/L \ll 1$ the motions are largely horizontal, and an expansion in the Rossby number Ro leads at second order to the standard quasi-geostrophic description in which vertical motions are largely (but not completely) suppressed. A similar analysis is possible when the aspect ratios A_y, A_z are of order one. In this case larger vertical motions are permitted, and closed equations can be derived by appropriately linking the Froude and buoyancy numbers to the Rossby number. We have termed the resulting equations the tilted quasi-hydrostatic quasi-geostrophic equations (TQH-QGE) (see Embid & Majda 1998). The final case where closed reduced equations were found is the case $A_z \gg 1$, in which motions take the form of slender rising and falling plumes. Here three classes of reduced equations were identified.

The first class, obtained for $A_z = o(Ro^{-1})$, represents a spatial extension of classical QG to tall columnar motions. The remaining two classes permit non-hydrostatic motions, and the interaction between vortical modes and inertial-gravity waves. These classes are distinguished by the magnitude of the Froude number. When Fr is small enough the mean stratification remains unchanged. In contrast, for larger Fr the motions feed back and change the mean stratification. The resulting equations are related to the reduced equations for rapidly rotating convection on the f -plane derived by Julien & Knobloch (1998). The derivation of these equations (for both hydrostatic and non-hydrostatic motions) using non-orthogonal coordinates as described in the present paper, enabled us to express the resulting equations in differential form, in contrast to Julien & Knobloch (1998) who employed Cartesian coordinates and could only write the reduced equations in Fourier space. The resulting equations describe the stretching of vorticity along the rotation vector by motions parallel to this vector, and the feedback of this mechanism on these motions. The process is driven by buoyancy, which has components both parallel and perpendicular to the local rotation vector, and opposed by viscous and thermal dissipation. Since the Taylor–Proudman constraint is implicitly taken into account, the resulting equations are amenable to efficient numerical techniques. These issues do not arise at the North Pole for which the corresponding equations were derived (and simulated) by Julien *et al.* (1998a), and by Sprague *et al.* (2006). In contrast at the equator the primary balance corresponds to sideways geostrophic balance, and the inclusion of a large scale in the meridional direction enabled us to capture the β -effect.

In each case we examined the conserved quantities, assuming that dissipative effects are negligible. This allowed us to examine the form of the potential vorticity conserved by the reduced equations in each regime, and to write down conserved Eulerian integrals, albeit under additional assumptions. The different forms of potential vorticity can be identified by an appropriate expansion of the general expression for potential vorticity (see Appendix B), but it is also necessary to check that the resulting expression is conserved by the corresponding reduced equations. The fact that in all cases the reduced potential vorticity is indeed conserved identifies the reduced potential vorticity as a fundamental quantity that restricts the dynamics of this type of system. We anticipate therefore that the reduced potential vorticity will play the role of a ‘slow mode’ once dissipation and weak forcing are taken into account, much as occurs in classical hydrostatic and quasi-hydrostatic QG models

where the potential vorticity determines the geostrophic streamfunction (Pedlosky 1979; Warn *et al.* 1995; Vallis 1996; Embid & Majda 1998).

It is of interest to understand the mechanisms whereby geostrophy breaks down as the leading-order balance. Such breakdown occurs when the criteria summarized in §§2.3.1–2.3.3 for geostrophic balance in equations (2.25) are violated. In the upright regime with $A_y \sim 1$ this occurs when $Ro/\eta_3 \gtrsim O(1)$. In the extratropics this condition implies that $Ro \gtrsim 1$. If $A_z \sim 1$ no reduction of the incompressible Navier–Stokes equations is then possible; however, if $A_z = o(1)$ the hydrostatic primitive equations (Salmon 1998) without a planetary β result. In the tropics where $\eta_3 \rightarrow 0$, it is possible to have $Ro = o(1)$, but non-geostrophic motion provided $A_z \lesssim O(Ro)$. In this situation, the primitive equations may be extended to include the equatorial β -effect resulting in the equatorial β -plane equations (Gill 1982) when $A_\beta \sim Ro$. No reduction is possible in the tilted and sideways regimes once geostrophy breaks down.

Although some of the equations we have derived here are known, the systematic derivation employed sheds new light on their origin and range of validity (cf. Majda & Klein 2003). In other cases our procedure led us to identify new classes of reduced equations governing rotationally constrained flows. This is the case particularly in the equatorial regions, and elsewhere in the non-hydrostatic regime. The latter is typically restricted to the oceanic case where the Boussinesq approximation is appropriate. For hydrostatic or non-hydrostatic fluid motions occurring in layers sufficiently deep that compressible effects become important, the anelastic approximation (Gough 1969; Bannon 1996) provides a better approximation. Extension of the theory presented here to this situation is therefore of importance for rotationally constrained motions occurring in the atmosphere, and the interiors of giant planets and stars. For upright non-hydrostatic motions, such an extension has been carried out (Julien *et al.* 1998*b*). These and other extensions of our approach will be reported in a future publication.

This work was supported by the National Science Foundation under Collaborative Grant NSF OCE 0137347/0137166. K. J. acknowledges partial financial support from a University of Colorado Faculty Fellowship Award. We are grateful to N. Pinardi, M. Sprague, G. Vallis and J. Weiss for helpful discussions.

Appendix A. Non-orthogonal coordinate systems

In this Appendix we provide a summary of the relevant identities required for the transformation between orthogonal Cartesian space with base vectors $\{\hat{\mathbf{e}}_1, \hat{\mathbf{e}}_2, \hat{\mathbf{e}}_3\} \equiv \{\hat{\mathbf{x}}, \hat{\mathbf{y}}, \hat{\mathbf{z}}\}$ and the non-orthogonal space with covariant base vectors $\{\hat{\mathbf{g}}_1, \hat{\mathbf{g}}_2, \hat{\mathbf{g}}_3\}$ (Aris 1962). Two possibilities arise:

Case A: $\{\hat{\mathbf{g}}_1, \hat{\mathbf{g}}_2, \hat{\mathbf{g}}_3\} \equiv \{\hat{\mathbf{x}}, \hat{\mathbf{y}}, \hat{\boldsymbol{\eta}}_0\}$ is appropriate for the tilted columnar motions in TH-QGE (table 4, equation (3.3); see also §6.1.1) and TNH-QGE I, II (table 4, equation (3.6); see also §6.1.2).

Case B: $\{\hat{\mathbf{g}}_1, \hat{\mathbf{g}}_2, \hat{\mathbf{g}}_3\} \equiv \{\hat{\mathbf{x}}, \hat{\boldsymbol{\eta}}_0, \hat{\mathbf{z}}\}$ is appropriate for the sideways columnar motions in TNH-QGE III (table 4, equation (6.1.2); see also §6.2).

Recall that the unit rotation vector is defined as $\hat{\boldsymbol{\eta}}_0 = \eta_2 \hat{\mathbf{y}} + \eta_3 \hat{\mathbf{z}}$, where $\eta_2 = \sin \vartheta$, $\eta_3 = \cos \vartheta$. The transformation between the Cartesian and non-orthogonal base vectors is given by $\hat{\mathbf{g}}_i = \mathbf{F} \hat{\mathbf{e}}_i$. Mappings between these coordinate representations follow from vector invariance

$$\mathbf{f} = r_1 \hat{\mathbf{x}} + r_2 \hat{\mathbf{y}} + r_3 \hat{\mathbf{z}} \equiv f^1 \hat{\mathbf{g}}_1 + f^2 \hat{\mathbf{g}}_2 + f^3 \hat{\mathbf{g}}_3, \quad (f^1, f^2, f^3)^T = \mathbf{F}^{-1} (r_1, r_2, r_3)^T, \quad (\text{A } 1)$$

where the f^i are the contravariant vector components associated with the non-orthogonal covariant base vectors. Also required are the contravariant (or dual) base vectors $\{\widehat{\mathbf{g}}^1, \widehat{\mathbf{g}}^2, \widehat{\mathbf{g}}^3\}$ with $\widehat{\mathbf{g}}^i = (\mathbf{F}^{-1})^T \widehat{\mathbf{e}}_i$ and $\mathbf{g}^i \mathbf{g}_j = \delta^i_j$. Here

$$\mathbf{f} = r_1 \widehat{\mathbf{x}} + r_2 \widehat{\mathbf{y}} + r_3 \widehat{\mathbf{z}} \equiv f_1 \widehat{\mathbf{g}}^1 + f_2 \widehat{\mathbf{g}}^2 + f_3 \widehat{\mathbf{g}}^3, \quad (f_1, f_2, f_3)^T = \mathbf{F}^T (r_1, r_2, r_3)^T. \quad (\text{A } 2)$$

Case A: $\{\widehat{\mathbf{g}}_1, \widehat{\mathbf{g}}_2, \widehat{\mathbf{g}}_3\} \equiv \{\widehat{\mathbf{x}}, \widehat{\mathbf{y}}, \widehat{\boldsymbol{\eta}}_0\}$

We denote the contravariant position and velocity coordinates in the non-orthogonal coordinate frame by $\mathbf{f} = (\tilde{x}, \tilde{y}, \eta)$ and $\mathbf{u} = (\tilde{u}, \tilde{v}, \tilde{w})$. The transformation matrix is given by

$$\mathbf{F} = \begin{pmatrix} 1 & 0 & 0 \\ 0 & 1 & \eta_2 \\ 0 & 0 & \eta_3 \end{pmatrix}, \quad \mathbf{F}^{-1} = \begin{pmatrix} 1 & 0 & 0 \\ 0 & 1 & -\frac{\eta_2}{\eta_3} \\ 0 & 0 & \frac{1}{\eta_3} \end{pmatrix}. \quad (\text{A } 3)$$

The columns of \mathbf{F} represent the non-orthogonal basis vectors $(\widehat{\mathbf{x}}, \widehat{\mathbf{y}}, \widehat{\boldsymbol{\eta}}_0)$ in Cartesian coordinates. Similarly, the rows of \mathbf{F}^{-1} represent the non-orthogonal dual basis vectors $(\widehat{\mathbf{g}}^1, \widehat{\mathbf{g}}^2, \widehat{\mathbf{g}}^3)$.

The relevant vector relations for deriving the reduced equations in the extratropical region are

$$\mathbf{f} \cdot \mathbf{h} = f^1 h_1 + f^2 h_2 + f^3 h_3 = f_1 h^1 + f_2 h^2 + f_3 h^3, \quad (\text{A } 4)$$

$$\begin{aligned} \nabla s &= \partial_{\tilde{x}} s \widehat{\mathbf{x}} + \left(\frac{1}{\eta_3^2} \partial_{\tilde{y}} - \frac{\eta_2}{\eta_3^2} \partial_{\eta} \right) s \widehat{\mathbf{y}} + \left(-\frac{\eta_2}{\eta_3^2} \partial_{\tilde{y}} + \frac{1}{\eta_3^2} \partial_{\eta} \right) s \widehat{\boldsymbol{\eta}}_0 \\ &= \partial_{\tilde{x}} s \widehat{\mathbf{g}}^1 + \partial_{\tilde{y}} s \widehat{\mathbf{g}}^2 + \partial_{\eta} s \widehat{\mathbf{g}}^3, \end{aligned}$$

$$\nabla \cdot \mathbf{f} = \partial_{\tilde{x}} f^1 + \partial_{\tilde{y}} f^2 + \partial_{\eta} f^3,$$

$$\mathbf{f} \cdot \nabla = f^1 \partial_{\tilde{x}} + f^2 \partial_{\tilde{y}} + f^3 \partial_{\eta},$$

$$\nabla^2 s \equiv \nabla_{\perp}^2 s = \left(\partial_{\tilde{x}}^2 + \frac{1}{\eta_3^2} \partial_{\tilde{y}}^2 - 2 \frac{\eta_2}{\eta_3^2} \partial_{\tilde{y}\eta}^2 + \frac{1}{\eta_3^2} \partial_{\eta}^2 \right) s,$$

$$\nabla \times \mathbf{f} = \frac{1}{\eta_3} \begin{vmatrix} \widehat{\mathbf{x}} & \widehat{\mathbf{y}} & \widehat{\boldsymbol{\eta}}_0 \\ \partial_{\tilde{x}} & \partial_{\tilde{y}} & \partial_{\eta} \\ f^1 & f^2 + \eta_2 f^3 & \eta_2 f^2 + f^3 \end{vmatrix},$$

$$\mathbf{f} \times \mathbf{h} = \frac{1}{\eta_3} \begin{vmatrix} \widehat{\mathbf{x}} & \widehat{\mathbf{y}} & \widehat{\boldsymbol{\eta}}_0 \\ f^1 & f^2 + \eta_2 f^3 & \eta_2 f^2 + f^3 \\ h^1 & h^2 + \eta_2 h^3 & \eta_2 h^2 + h^3 \end{vmatrix}.$$

The dot products above require knowledge of both contravariant and covariant coordinates. For this reason ∇s is given in both the non-orthogonal coordinate system and in its dual space. The following results are also useful: $\widehat{\boldsymbol{\eta}}_0 = (0, 0, 1)$ in $(\widehat{\mathbf{x}}, \widehat{\mathbf{y}}, \widehat{\boldsymbol{\eta}}_0)$ and $\widehat{\boldsymbol{\eta}}_0 = (0, \eta_2, 1)$ in $(\widehat{\mathbf{g}}^1, \widehat{\mathbf{g}}^2, \widehat{\mathbf{g}}^3)$.

Modulation

The Taylor–Proudman constraint implies that $\partial/\partial\eta \equiv 0$ on small scales. However, on large scales in the $\widehat{\boldsymbol{\eta}}_0$ direction, inhomogeneities must be permitted. We therefore let $\partial_{\eta} \rightarrow A_{\chi}^{-1} \partial_{\chi}$, where $\chi = \eta/A_{\chi}$ and $A_{\chi} = L_{\chi}/L \gg 1$. Expression (A 4b) implies that

this modulation changes the gradient vector by

$$\frac{1}{A_x} \left(-\frac{\eta_2}{\eta_3} \hat{\mathbf{y}} + \frac{1}{\eta_3} \hat{\boldsymbol{\eta}}_0 \right) \partial_x \equiv \frac{1}{A_x} \hat{\mathbf{z}} \partial_x \equiv \frac{1}{A_z} \hat{\mathbf{z}} \partial_z, \tag{A 5}$$

where the latter identity follows from $L_\eta = \eta_3 L_z$ and $Z = \eta_3 \chi$. Thus the net effect of the modulation is to describe large-scale modulation in the local vertical direction. However, as $\eta_3 \rightarrow 0$ this non-orthogonal system becomes degenerate and $L_x \rightarrow \infty$. We therefore consider the following case as well.

Case B: $\{\hat{\mathbf{g}}_1, \hat{\mathbf{g}}_2, \hat{\mathbf{g}}_3\} \equiv \{\hat{\mathbf{x}}, \hat{\boldsymbol{\eta}}_0, \hat{\mathbf{z}}\}$

The contravariant position and velocity coordinates in this non-orthogonal frame are given by $\mathbf{f} = (\tilde{x}, \eta, \tilde{z})$ and $\mathbf{u} = (\tilde{u}, \tilde{v}, \tilde{w})$. The transformation matrix is given by

$$\mathbf{F} = \begin{pmatrix} 1 & 0 & 0 \\ 0 & \eta_2 & 0 \\ 0 & \eta_3 & 1 \end{pmatrix}, \quad \mathbf{F}^{-1} = \begin{pmatrix} 1 & 0 & 0 \\ 0 & \frac{1}{\eta_2} & 0 \\ 0 & -\frac{\eta_3}{\eta_2} & 1 \end{pmatrix}. \tag{A 6}$$

The columns of \mathbf{F} and rows of \mathbf{F}^{-1} represent the non-orthogonal basis vectors and their dual vectors, respectively.

Near the tropics the relevant position variables are $(\tilde{x}, Y, \tilde{z})$ and the vector relations for deriving reduced equations are

$$\begin{aligned} \mathbf{f} \cdot \mathbf{h} &= f^1 h_1 + f^2 h_2 + f^3 h_3 = f_1 h^1 + f_2 h^2 + f_3 h^3, \\ \nabla s &= \partial_{\tilde{x}} s \hat{\mathbf{x}} + \left(\frac{1}{\eta_2} \partial_\eta - \frac{\eta_3}{\eta_2} \partial_{\tilde{z}} \right) s \hat{\boldsymbol{\eta}}_0 + \left(-\frac{\eta_3}{\eta_2} \partial_\eta + \frac{1}{\eta_2} \partial_{\tilde{z}} \right) s \hat{\mathbf{z}} \\ &= \partial_{\tilde{x}} s \hat{\mathbf{g}}^1 + \partial_\eta s \hat{\mathbf{g}}^2 + \partial_{\tilde{z}} s \hat{\mathbf{g}}^3, \\ \nabla \cdot \mathbf{f} &= \partial_{\tilde{x}} f^1 + \partial_\eta f^2 + \partial_{\tilde{z}} f^3, \\ \mathbf{f} \cdot \nabla &= f^1 \partial_{\tilde{x}} + f^2 \partial_\eta + f^3 \partial_{\tilde{z}}, \\ \nabla^2 s &= \left(\partial_{\tilde{x}}^2 + \frac{1}{\eta_2^2} \partial_\eta^2 - 2 \frac{\eta_3}{\eta_2^2} \partial_{\eta \tilde{z}}^2 + \frac{1}{\eta_2^2} \partial_{\tilde{z}}^2 \right) s, \\ \nabla \times \mathbf{f} &= \frac{1}{\eta_2} \begin{vmatrix} \hat{\mathbf{x}} & \hat{\boldsymbol{\eta}}_0 & \hat{\mathbf{z}} \\ \partial_{\tilde{x}} & \partial_\eta & \partial_{\tilde{z}} \\ f^1 & f^2 + \eta_3 f^3 & \eta_3 f^2 + f^3 \end{vmatrix}, \\ \mathbf{f} \times \mathbf{h} &= \frac{1}{\eta_2} \begin{vmatrix} \hat{\mathbf{x}} & \hat{\boldsymbol{\eta}}_0 & \hat{\mathbf{z}} \\ f^1 & f^2 + \eta_3 f^3 & \eta_3 f^2 + f^3 \\ h^1 & h^2 + \eta_3 h^3 & \eta_3 h^2 + h^3 \end{vmatrix}. \end{aligned}$$

Note that $\hat{\boldsymbol{\eta}}_0 = (0, 1, 0)$ in $(\hat{\mathbf{x}}, \hat{\boldsymbol{\eta}}_0, \hat{\mathbf{z}})$ and $\hat{\boldsymbol{\eta}}_0 = (0, 1, \eta_3)$ in $(\hat{\mathbf{g}}^1, \hat{\mathbf{g}}^2, \hat{\mathbf{g}}^3)$.

Modulation

Modulation along the $\hat{\boldsymbol{\eta}}_0$ direction translates into the change

$$\frac{1}{A_x} \left(\frac{1}{\eta_2^2} \hat{\boldsymbol{\eta}}_0 - \frac{\eta_3}{\eta_2^2} \hat{\mathbf{z}} \right) \partial_x \equiv \frac{1}{A_Y} \hat{\mathbf{y}} \partial_Y \tag{A 7}$$

in the gradient operator ∇ , and so corresponds to modulation in the meridional direction $\hat{\mathbf{y}}$. Here $A_x = L_x/L$ and $L_x = \eta_2 L_y, Y = \eta_2 \chi$.

Appendix B. Potential vorticity

In this Appendix, we derive the different forms of the conserved potential vorticity found above using an asymptotic expansion of the general conservation law

$$D_t(\boldsymbol{\omega}_a \cdot \nabla \Pi) = -Ro^{-1} A_\beta \eta_3 \nabla \cdot (\mathbf{u} \Pi), \quad (\text{B } 1)$$

where $\boldsymbol{\omega}_a = \boldsymbol{\omega} + Ro^{-1} \boldsymbol{\Omega}(y)$, $\boldsymbol{\Omega}(y) = \widehat{\boldsymbol{\eta}}_0 - A_\beta y \widehat{\boldsymbol{\eta}}_1$, and $\Pi = b - \mathcal{F}^{-2} \bar{\rho}$. Such a derivation is, in general, simpler than direct computation using the reduced equations, but we emphasize that the latter is, in general, necessary since the order to which a truncated form of the potential vorticity will be conserved by given reduced equations cannot be known *a priori*.

B.1. The case UH-QGE

We consider the parameter values given in table 3, row 1, with $\mathcal{F} = \epsilon^{1/2}$ and $A_z \ll 1$ as appropriate for the extratropics. The relative and planetary vorticities then decompose into several terms of differing asymptotic magnitude:

$$\boldsymbol{\omega} = \frac{1}{A_z} \begin{pmatrix} -\partial_z v \\ \partial_z u \\ 0 \end{pmatrix} + \begin{pmatrix} 0 \\ 0 \\ \partial_x v - \partial_y u \end{pmatrix} + A_z \begin{pmatrix} \partial_y w \\ -\partial_x w \\ 0 \end{pmatrix} \equiv \frac{1}{A_z} \boldsymbol{\omega}^L + \boldsymbol{\omega}^N + A_z \boldsymbol{\omega}^S,$$

$$\boldsymbol{\Omega}(y) = \widehat{\boldsymbol{\eta}}_0 - \epsilon \beta y \widehat{\boldsymbol{\eta}}_1.$$

A substitution of this result into the exact conservation law (B 1) together with a double asymptotic expansion,

$$\mathbf{v} = \sum_{i,j} \epsilon^i A_z^j \mathbf{v}_{ij}, \quad \mathbf{v}_{00} \equiv \mathbf{v}_0, \quad (\text{B } 2)$$

for all fields now yields the following order by order requirements ($\Pi_{-10} = -\bar{\rho}(z)$, $\Pi_{ij} = b_{ij}$):

$$O(\epsilon^{-1} A_z^{-2}): \quad D_t^{00} [(\boldsymbol{\omega}_{00}^L \cdot \widehat{\mathbf{z}}) \partial_z \Pi_{-10}] = 0,$$

$$O(\epsilon^{-2} A_z^{-1}): \quad D_t^{00} [(\widehat{\boldsymbol{\eta}}_0 \cdot \widehat{\mathbf{z}}) \partial_z \Pi_{-10}] = 0,$$

$$O(\epsilon^{-2}): \quad D_t^{00} [(\widehat{\boldsymbol{\eta}}_0 \cdot \nabla_\perp) \Pi_{-10}] = 0,$$

$$O(A_z^{-2}): \quad D_t^{00} [(\boldsymbol{\omega}_{00}^L \cdot \widehat{\mathbf{z}}) \partial_z \Pi_{00}] = 0,$$

where $D_t^{00} = \partial_t + \mathbf{u}_{00\perp} \cdot \nabla_\perp$ since the vertical velocity $w_{00} \equiv 0$. All of these are trivially satisfied. At $O(\epsilon^{-1} A_z^{-1})$, we obtain

$$D_t^{00} [(\boldsymbol{\omega}_{00}^L \cdot \nabla_\perp) \Pi_{-10} + (\boldsymbol{\omega}_{00}^N \cdot \widehat{\mathbf{z}}) \partial_z \Pi_{-10} + (\widehat{\boldsymbol{\eta}}_0 \cdot \widehat{\mathbf{z}}) \partial_z \Pi_{00} - \beta y (\widehat{\boldsymbol{\eta}}_1 \cdot \widehat{\mathbf{z}}) \partial_z \Pi_{-10}] \\ + D_t^{00} [(\boldsymbol{\omega}_{01}^L \cdot \widehat{\mathbf{z}}) \partial_z \Pi_{-10}] + D_t^{01} [(\boldsymbol{\omega}_{00}^L \cdot \widehat{\mathbf{z}}) \partial_z \Pi_{-10}] + D_t^{10} [(\widehat{\boldsymbol{\eta}}_0 \cdot \widehat{\mathbf{z}}) \partial_z \Pi_{-10}] = 0,$$

where, for $i, j \neq 0$, $D_t^{ij} = \mathbf{u}_{ij} \cdot \nabla$. This equation readily simplifies to

$$D_t^{00} [(\boldsymbol{\omega}_0^N \cdot \widehat{\mathbf{z}}) \partial_z \Pi_{-10} + (\widehat{\boldsymbol{\eta}}_0 \cdot \widehat{\mathbf{z}}) \partial_z \Pi_{00} - \beta y (\widehat{\boldsymbol{\eta}}_1 \cdot \widehat{\mathbf{z}}) \partial_z \Pi_{-10}] + w_{10} \partial_z [(\widehat{\boldsymbol{\eta}}_0 \cdot \widehat{\mathbf{z}}) \partial_z \Pi_{-10}] = 0. \quad (\text{B } 3)$$

In addition, the buoyancy equation (4.10) implies

$$w_{10} = -D_t^{00} \left(\frac{\Pi_{00}}{\partial_z \Pi_{-10}} \right),$$

and since $\Pi_0 \equiv b_0 = (\hat{\boldsymbol{\eta}} \cdot \hat{\mathbf{z}}) \partial_z \Psi_{00}$, the potential vorticity equation (B 3) collapses to

$$D_t^{00} \left[\boldsymbol{\omega}_{00}^N \cdot \hat{\mathbf{z}} - (\hat{\boldsymbol{\eta}}_0 \cdot \hat{\mathbf{z}}) \partial_z \left(\frac{(\hat{\boldsymbol{\eta}}_0 \cdot \hat{\mathbf{z}}) \partial_z \Psi_{00}}{\partial_z \bar{\rho}(z)} \right) - \beta y (\hat{\boldsymbol{\eta}}_1 \cdot \hat{\mathbf{z}}) \right] = 0, \quad (\text{B } 4)$$

as obtained in table 4, equation (3.1c).

B.2. The case TQH-QGE

We assume the distinguished parameter values given in table 3, row 2, with $\mathcal{F} = \epsilon^{1/2}$. The relative and planetary vorticities are

$$\boldsymbol{\omega} = \nabla \times \mathbf{u}, \quad \boldsymbol{\Omega}(y) = \hat{\boldsymbol{\eta}}_0 - \epsilon \beta y \hat{\boldsymbol{\eta}}_1.$$

We substitute this result together with expansions of the form

$$\mathbf{v} = \sum_i \epsilon^i \mathbf{v}_i$$

of all the fields into equation (B 1), and write $\Pi_{-1} = -\bar{\rho}(z)$ and $\Pi_i = b_i$. Then at $O(\epsilon^{-2})$

$$D_t^0 [(\hat{\boldsymbol{\eta}}_0 \cdot \nabla) \Pi_{-1}] = 0,$$

where $D_t^i = \partial_t + \mathbf{u}_i \cdot \nabla$. This equation is trivially satisfied because $w_0 \equiv 0$ and $D_t^0 \Pi_{-1} \equiv 0$. At $O(\epsilon^{-1})$, we obtain

$$D_t^0 [(\boldsymbol{\omega}_0 \cdot \nabla) \Pi_{-1} + (\hat{\boldsymbol{\eta}}_0 \cdot \nabla) \Pi_0 - \beta y (\hat{\boldsymbol{\eta}}_1 \cdot \nabla) \Pi_{-1}] + D_t^1 [(\hat{\boldsymbol{\eta}}_0 \cdot \nabla) \Pi_{-1}] = 0,$$

or, equivalently,

$$D_t^0 [(\boldsymbol{\omega}_0 \cdot \nabla) \Pi_{-1} + (\hat{\boldsymbol{\eta}}_0 \cdot \nabla) \Pi_0 - \beta y (\hat{\boldsymbol{\eta}}_1 \cdot \nabla) \Pi_{-1}] + w_1 \partial_z [(\hat{\boldsymbol{\eta}}_0 \cdot \nabla) \Pi_{-1}] = 0, \quad (\text{B } 5)$$

while from the buoyancy equation (§ 5, equation (5.8)) we obtain

$$w_1 = -D_t^0 \left(\frac{\Pi_0}{\partial_z \Pi_{-1}} \right).$$

Since $\Pi_0 \equiv b_0 = (\hat{\boldsymbol{\eta}} \cdot \nabla) \Psi_0$, the potential vorticity equation (B 5) collapses to

$$D_t^0 \left[\boldsymbol{\omega}_0 \cdot \hat{\mathbf{z}} - (\hat{\boldsymbol{\eta}}_0 \cdot \nabla) \left(\frac{(\hat{\boldsymbol{\eta}}_0 \cdot \nabla) \Psi_0}{\partial_z \bar{\rho}(z)} \right) - \beta y (\hat{\boldsymbol{\eta}}_1 \cdot \hat{\mathbf{z}}) \right] = 0, \quad (\text{B } 6)$$

as obtained in equation (6.34). Note that the TQH-QGE become UH-QGE as $\hat{\boldsymbol{\eta}}_0 \rightarrow \hat{\mathbf{z}}$, an observation that can be used to establish conservation of potential vorticity for the latter system.

B.3. The case TH-QGE

This case is characterized by the parameter values in table 3, row 3. The relative and planetary vorticities are

$$\boldsymbol{\omega}' = (\nabla + A_Z^{-1} \hat{\mathbf{z}} \partial_z) \times \mathbf{u}' \equiv \boldsymbol{\omega}^N + A_Z^{-1} \boldsymbol{\omega}^S, \quad \boldsymbol{\Omega}(y) = \hat{\boldsymbol{\eta}}_0.$$

Although $1 < A_Z < O(Ro^{-1})$, for brevity we treat only the case $A_Z = \epsilon^{-1/2}$ and assume that $\mathcal{F} = \epsilon^{1/2}$. These relations suggest that we expand all fields in powers of $\epsilon^{1/2}$,

$$\mathbf{v} = \sum_i \epsilon^{i/2} \mathbf{v}_{i/2}.$$

At $O(\epsilon^{-2})$, equation (B 1) yields

$$D_t^0 [(\hat{\boldsymbol{\eta}}_0 \cdot \nabla) \Pi_{-1}] = 0.$$

This equation is trivially satisfied since $\Pi_{-1} = -\bar{\rho}(Z)$. At $O(\epsilon^{-3/2})$, we find

$$D_t^0[(\hat{\eta}_0 \cdot \hat{z})\partial_Z \Pi_{-1}] + D_t^{1/2}[(\hat{\eta}_0 \cdot \nabla)\Pi_{-1}] + (\mathbf{u}'_0 \cdot \hat{z})\partial_Z[(\hat{\eta}_0 \cdot \nabla)\Pi_{-1}] = 0,$$

which is also trivially satisfied since $\nabla \Pi_{-1} = 0$. At $O(\epsilon^{-1})$, we find

$$D_t^0[(\hat{\eta}_0 \cdot \nabla)\Pi_0] + (\mathbf{u}'_0 \cdot \hat{z})\partial_Z[(\hat{\eta}_0 \cdot \hat{z})\partial_Z \Pi_{-1}] = 0,$$

where $\Pi_0 = b'_0$. The Taylor–Proudman constraint $\hat{\eta}_0 \cdot \nabla \Pi_0 = 0$ together with the fact that $w_0 = 0$ shows that this relation is also trivially satisfied. At $O(\epsilon^{-1/2})$ we finally obtain

$$D_t^0[(\hat{\eta}_0 \cdot \nabla)\Pi_{1/2} + (\hat{\eta}_0 \cdot \hat{z})\partial_Z \Pi_0 + (\boldsymbol{\omega}_0^N \cdot \hat{z})\partial_Z \Pi_{-1}] + (\mathbf{u}'_{1/2} \cdot \hat{z})\partial_Z[(\hat{\eta}_0 \cdot \hat{z})\partial_Z \Pi_{-1}] = 0.$$

The unknown quantity $\Pi_{1/2}$ can be eliminated by averaging this equation in η and using the fact that $\partial_\eta(\mathbf{u}'_{1/2} \cdot \hat{z}) = 0$. Thus,

$$D_t^0[(\hat{\eta}_0 \cdot \hat{z})\partial_Z \Pi_0 + (\boldsymbol{\omega}_0^N \cdot \hat{z})\partial_Z \Pi_{-1}] + (\mathbf{u}'_{1/2} \cdot \hat{z})\partial_Z[(\hat{\eta}_0 \cdot \hat{z})\partial_Z \Pi_{-1}] = 0.$$

From the buoyancy equation (6.17) we obtain

$$w'_{1/2} = -D_t^0 \left(\frac{\Pi_0}{\partial_Z \Pi_{-1}} \right),$$

and upon noting the closure $\Pi_0 \equiv b'_0 = \partial_Z \Psi_0$, the potential vorticity equation collapses to

$$D_t^0 \left[\boldsymbol{\omega}_0^N \cdot \hat{z} - (\hat{\eta}_0 \cdot \hat{z})\partial_Z \left(\frac{\partial_Z \Psi_0}{\partial_Z \bar{\rho}(Z)} \right) \right] = 0, \quad (\text{B } 7)$$

as obtained in equation (3.3c).

B.4. The cases TNH-QGE I, II

We derive here the potential vorticity for TNH-QGE II for the distinguished parameters given in table 3, row 5. The calculation for TNH-QGE I is very similar and is therefore omitted. The vorticity is given by

$$\boldsymbol{\omega}' = (\nabla + \epsilon \hat{z} \partial_Z) \times \mathbf{u}' \equiv \boldsymbol{\omega}^N + \epsilon \boldsymbol{\omega}^S, \quad \boldsymbol{\Omega}(y) = \hat{\eta}_0.$$

Here the β -effect is negligible. The conservation of potential vorticity then becomes

$$D_t[(\boldsymbol{\omega}_a \cdot \nabla)\Pi] \equiv (D_t + \epsilon^2 \partial_T + \epsilon \hat{z} \cdot \mathbf{u}' \partial_Z)[(\boldsymbol{\omega}_a \cdot \nabla)\Pi] = 0.$$

At $O(\epsilon^{-1})$ we obtain

$$D_t^0[(\hat{\eta}_0 \cdot \nabla)\Pi_0] = 0,$$

a relation that is trivially satisfied given that $\Pi_0 = \bar{b}_0(Z) - \mathcal{F}^{-2}\bar{\rho}(Z)$ and $\nabla \Pi_0 \equiv 0$. At $O(1)$ we obtain

$$D_t^0[(\boldsymbol{\omega}_0^N \cdot \nabla)\Pi_0 + (\hat{\eta}_0 \cdot \hat{z})\partial_Z \Pi_0] + D_t^1[(\hat{\eta}_0 \cdot \nabla)\Pi_0] + (\mathbf{u}'_0 \cdot \hat{z})\partial_Z[(\hat{\eta}_0 \cdot \nabla)\Pi_0] = 0,$$

where we have used the fact that $\hat{\eta}_0 \cdot \nabla b'_1 = 0$ and the approximation $\mathbf{u}_0 \approx \mathbf{u}'_0$. The resulting expression is trivially satisfied since $\nabla \Pi_0 \equiv 0$. Using this fact we obtain at $O(\epsilon)$

$$\begin{aligned} & D_t^0[(\boldsymbol{\omega}_0^N \cdot \nabla)\Pi_1 + (\boldsymbol{\omega}_0^N \cdot \hat{z})\partial_Z \Pi_0 + (\hat{\eta}_0 \cdot \nabla)\Pi_2 + (\hat{\eta}_0 \cdot \hat{z})\partial_Z \Pi_1] \\ & + D_t^1[(\hat{\eta}_0 \cdot \hat{z})\partial_Z \Pi_0 + (\hat{\eta}_0 \cdot \nabla)\Pi_1] + (\hat{z} \cdot \mathbf{u}'_0)\partial_Z[(\hat{\eta}_0 \cdot \hat{z})\partial_Z \Pi_0 + (\hat{\eta}_0 \cdot \nabla)\Pi_1] = 0, \end{aligned}$$

where $D_t^1 = \mathbf{u}'_1 \cdot \nabla$, $\Pi_1 = b'_1$ and $\Pi_2 = b'_2$. The unknown quantity Π_2 can be eliminated by averaging this equation in η . On using the Taylor–Proudman constraint $\hat{\boldsymbol{\eta}}_0 \cdot \nabla \equiv 0$ this averaged equation reduces to

$$D_t^0 [(\boldsymbol{\omega}_0^N \cdot \nabla) \Pi_1 + (\boldsymbol{\omega}_0^N \cdot \hat{\mathbf{z}}) \partial_z \Pi_0 + (\hat{\boldsymbol{\eta}}_0 \cdot \hat{\mathbf{z}}) \partial_z \Pi_1] + (\hat{\mathbf{z}} \cdot \mathbf{u}'_0) \partial_z (\hat{\boldsymbol{\eta}}_0 \cdot \hat{\mathbf{z}}) \partial_z \Pi_0 = 0.$$

From the buoyancy equation (6.32*b*), we obtain

$$\hat{\mathbf{z}} \cdot \mathbf{u}'_0 = -D_t^0 \left(\frac{\Pi_1}{\partial_z \Pi_0} \right),$$

and the potential vorticity equation therefore collapses to

$$D_t^0 \left[\boldsymbol{\omega}_0^N \cdot \hat{\mathbf{z}} + (\boldsymbol{\omega}_0^N \cdot \nabla + \hat{\boldsymbol{\eta}}_0 \cdot \hat{\mathbf{z}} \partial_z) \left(\frac{\Pi_1}{\partial_z \Pi_0} \right) \right] = 0. \quad (\text{B } 8)$$

The derivation of the potential vorticity equation for TNH-QGE I is identical to the above derivation, except that the leading-order term is now ϵ^{-2} and $\Pi_0 = -\mathcal{F}^2 \bar{\rho}(Z)$, $\Pi_1 = b'_0$, and $\Pi_2 = b'_1$.

B.5. The case TNH-QGE III

The distinguished parameters for this case are given in table 3; the system SNH-QGE is obtained in the limit $\hat{\boldsymbol{\eta}}_0 \rightarrow \hat{\mathbf{y}}$. The relative and planetary vorticities are given by

$$\boldsymbol{\omega}' = (\nabla + \epsilon \hat{\mathbf{y}} \partial_y) \times \mathbf{u}' \equiv \boldsymbol{\omega}^N + \epsilon \boldsymbol{\omega}^S, \quad \boldsymbol{\Omega}(Y) = \hat{\boldsymbol{\eta}}_0 - \epsilon \beta Y \hat{\boldsymbol{\eta}}_1.$$

At $O(\epsilon^{-1})$ we obtain

$$D_t^0 [(\hat{\boldsymbol{\eta}}_0 \cdot \nabla) \Pi_0] = 0,$$

where $\Pi_0 = b_0 - \mathcal{F}^{-2} \bar{\rho}(z)$. This condition is trivially satisfied since $(\hat{\boldsymbol{\eta}}_0 \cdot \nabla) \Pi_0 = 0$. The Taylor–Proudman constraint $\hat{\boldsymbol{\eta}}_0 \cdot \nabla \equiv 0$ at $O(1)$ implies

$$D_t^0 [(\hat{\boldsymbol{\eta}}_0 \cdot \nabla) \Pi_1 + (\boldsymbol{\omega}_0^N \cdot \nabla) \Pi_0 + (\hat{\boldsymbol{\eta}}_0 \cdot \hat{\mathbf{y}}) \partial_y \Pi_0 - \beta Y (\hat{\boldsymbol{\eta}}_1 \cdot \nabla) \Pi_0] = 0.$$

The quantity Π_1 can be eliminated upon averaging in η . We obtain

$$D_t^0 [(\boldsymbol{\omega}_0^N \cdot \nabla + \hat{\boldsymbol{\eta}}_0 \cdot \hat{\mathbf{y}} \partial_y - \beta Y \hat{\boldsymbol{\eta}}_1 \cdot \nabla) \Pi_0] = 0, \quad (\text{B } 9)$$

in agreement with equation (6.43).

REFERENCES

- ARIS, R. 1962 *Vectors, Tensors and Basic Equations of Fluid Mechanics*. Dover.
- AURNOU, J. M. & OLSON, P. L. 2001 Strong zonal winds from thermal convection in a rotating spherical shell. *Geophys. Res. Lett.* **28**, 2557–2559.
- BANNON, P. R. 1996 On the anelastic approximation for a compressible atmosphere. *J. Atmos. Sci.* **53**, 3618–3628.
- BOUBNOV, B. M. & GOLITSYN, G. S. 1990 Temperature and velocity field regimes of convective motions in a rotating plane fluid layer. *J. Fluid Mech.* **219**, 215–239.
- BUSSE, F. H. 1970 Thermal instabilities in rapidly rotating systems. *J. Fluid Mech.* **44**, 441–460.
- BUSSE, F. H. 2002 Convective flows in rapidly rotating spheres and their dynamo action. *Phys. Fluids* **14**, 1301–1314.
- CHARNEY, J. G. 1948 On the scale of atmospheric motions. *Geophys. Publ.* **17**, 3–17.
- CHARNEY, J. G. 1971 Geostrophic turbulence. *J. Atmos. Sci.* **28**, 1087–1095.
- EMBID, P. & MAJDA, A. J. 1998 Low Froude number limiting dynamics for stably stratified flow with small or finite Rossby numbers. *Geophys. Astrophys. Fluid Dyn.* **87**, 1–50.

- FERNANDO, H. J. S., CHEN, R. & BOYER, D. L. 1991 Effects of rotation on convection turbulence. *J. Fluid Mech.* **228**, 513–547.
- GILL, A. E. 1982 *Atmosphere–Ocean Dynamics*, International Geophysics Series **30**. Academic.
- GOUGH, D. O. 1969 The anelastic approximation for thermal convection. *J. Atmos. Sci.* **26**, 448–456.
- HART, J. E., GLATZMAIER, G. A. & TOOMRE, J. 1986 Space-laboratory and numerical simulations of thermal convection in a rotating hemispherical shell with radial gravity. *J. Fluid Mech.* **173**, 519–544.
- HART, J. E. & OHLSEN, D. R. 1999 On the thermal offset in turbulent rotating convection. *Phys. Fluids* **11**, 2101–2107.
- JULIEN, K. & KNOBLOCH, E. 1998 Strongly nonlinear convection cells in a rapidly rotating fluid layer: the tilted f -plane. *J. Fluid Mech.* **360**, 141–178.
- JULIEN, K., KNOBLOCH, E. & WERNE, J. 1998a A new class of equations for rotationally constrained flows. *J. Theor. Comp. Fluid Dyn.* **11**, 251–261.
- JULIEN, K., KNOBLOCH, E. & WERNE, J. 1998b Reduced equations for rotationally constrained convection. In *First International Symposium on Turbulence & Shear Flow Phenomena* (ed. S. Banerjee & J. K. Eaton), vol. 1, pp. 101–106. Begel House.
- JULIEN, K., LEGG, S., MCWILLIAMS, J. & WERNE, J. 1996a Penetrative convection in rapidly rotating flows: Preliminary results from numerical simulation. *Dyn. Atmos. Oceans* **24**, 237–249.
- JULIEN, K., LEGG, S., MCWILLIAMS, J. C. & WERNE, J. 1996b Rapidly rotating Rayleigh–Bénard convection. *J. Fluid Mech.* **322**, 243–273.
- LEVY, M. A. & FERNANDO, H. J. S. 2003 Turbulent thermal convection in a rotating stratified fluid. *J. Fluid Mech.* **467**, 19–40.
- LIU, Y. & ECKE, R. E. 1997 Heat transport scaling in turbulent Rayleigh–Bénard convection: Effects of rotation and Prandtl number. *Phys. Rev. Lett.* **79**, 2257–2260.
- MCWILLIAMS, J. C., WEISS, J. B. & YAVNEH, I. 1994 Anisotropy and coherent vortex structures in planetary turbulence. *Science*, **264**, 410–413.
- MCWILLIAMS, J. C., WEISS, J. B. & YAVNEH, I. 1999 The vortices of homogeneous geostrophic turbulence. *J. Fluid Mech.* **401**, 1–26.
- MADDEN, R. A. & JULIAN, P. 1972 Description of global scale circulation cells in the tropics with 40–50 day period. *J. Atmos. Sci.* **29**, 1109–1123.
- MADDEN, R. A. & JULIAN, P. 1994 Observations of the 40–50-day tropical oscillation – a review. *Mon. Weather Rev.* **122**, 814–837.
- MAJDA, A. J. & KLEIN, R. 2003 Systematic multiscale models for the tropics. *J. Atmos. Sci.* **60**, 393–408.
- MARSHALL, J. & SCHOTT, F. 1999 Open-ocean convection: observations, theory and models. *Rev. Geophys.* **37**, 1–64.
- MAXWORTHY, T. & NARIMOUSA, S. 1994 Unsteady, turbulent convection into a homogeneous, rotating fluid, with oceanographic application. *J. Phys. Oceanogr.* **24**, 865–887.
- OHLSEN, D. R., HART, J. E. & KITTELMAN, S. 1995 Laboratory experiments on rotating turbulent convection, *Am. Met. Soc. Tenth Conf. on Atmospheric and Oceanic Waves and Stability (Preprints)*, p. 255.
- PEDLOSKY, J. 1979 *Geophysical Fluid Dynamics*. Springer.
- PICKART, R. S., TORRES, D. J. & CLARKE, R. A. 2002 Hydrography of the Labrador Sea during active convection. *J. Phys. Oceanogr.* **32**, 428–457.
- PROUDMAN, J. 1916 On the motion of solids in a liquid possessing vorticity. *Proc. R. Soc. Lond. A* **92**, 408–424.
- SAKAI, S. 1997 The horizontal scale of rotating convection in the geostrophic regime. *J. Fluid Mech.* **333**, 85–95.
- SALMON, R. 1998. *Lecture Notes on Geophysical Fluid Dynamics*. Oxford University Press.
- SHEPHERD, T. G. 1993 A unified theory of available potential energy. *Atmos. Ocean*, **31**, 1–26.
- SMITH, L. M. & WALEFFE, F. 2002 Generation of slow large scales in forced rotating stratified turbulence. *J. Fluid Mech.* **451**, 145–168.
- SPRAGUE, M., JULIEN, K., KNOBLOCH, E. & WERNE, J. 2006 Numerical simulation of an asymptotically reduced system for rotationally constrained convection. *J. Fluid Mech.* **551**, 141–174.

- TAYLOR, G. I. 1923 Experiments on the motion of solid bodies in rotating fluids. *Proc. R. Soc. Lond. A* **104**, 213–218.
- VALLIS, G. K. 1996 Potential vorticity inversion and balanced equations of motion for rotating and stratified flows. *Q. J. R. Met. Soc.* **122**, 291–322.
- WARN, T., BOKHOVE, O., SHEPHERD, T. G. & VALLIS, G. K. 1995 Rossby number expansions, slaving principles, and balance dynamics. *Q. J. R. Met. Soc.* **121**, 723–739.
- WHITE, A. A. & BROMLEY, R. A. 1995 Dynamically consistent, quasi-hydrostatic equations for global models with a complete representation of the Coriolis force. *Q. J. R. Met. Soc.* **121**, 399–418.